



EPA Public Access

Author manuscript

Indoor Air. Author manuscript; available in PMC 2021 September 03.

About author manuscripts

Submit a manuscript

Published in final edited form as:

Indoor Air. 2019 September ; 29(5): 761–779. doi:10.1111/ina.12584.

Analysis of indoor particles and gases and their evolution with natural ventilation

Claire Fortenberry¹, Michael Walker¹, Audrey Dang¹, Arun Loka², Gauri Date², Karolina Cysneiros de Carvalho¹, Glenn Morrison^{2,3}, Brent Williams¹

¹Department of Energy, Environmental and Chemical Engineering, Washington University in St. Louis, St. Louis, Missouri

²Department of Civil, Architectural and Environmental Engineering, Missouri University of Science and Technology, Rolla, Missouri

³Department of Environmental Sciences and Engineering, University of North Carolina at Chapel Hill, Chapel Hill, North Carolina

Abstract

The air composition and reactivity from outdoor and indoor mixing field campaign was conducted to investigate the impacts of natural ventilation (ie, window opening and closing) on indoor air quality. In this study, a thermal desorption aerosol gas chromatograph (TAG) obtained measurements of indoor particle- and gas-phase semi- and intermediately volatile organic compounds both inside and outside a single-family test home. Together with measurements from a suite of instruments, we use TAG data to evaluate changes in indoor particles and gases at three natural ventilation periods. Positive matrix factorization was performed on TAG and adsorbent tube data to explore five distinct chemical and physical processes occurring in the indoor environment. Outdoor-to-indoor transport is observed for sulfate, isoprene epoxydiols, polycyclic aromatic hydrocarbons, and heavy alkanes. Dilution of indoor species is observed for volatile, non-reactive species including methylcyclohexane and decamethylcyclopentasiloxane. Window opening drives enhanced emissions of semi- and intermediately volatile species including TXIB, DEET, diethyl phthalate, and carvone from indoor surfaces. Formation via enhanced oxidation was observed for nonanal and 2-decanone when outdoor oxidants entered the home. Finally, oxidative depletion of gas-phase terpenes (eg, limonene and α -pinene) was anticipated but not observed due to limited measurement resolution and dynamically changing conditions.

Keywords

field measurements; gas chromatography-mass spectrometry; gas-particle partitioning; natural ventilation; residential air quality; semivolatile organic compounds

Correspondence: Brent Williams, Department of Energy, Environmental, and Chemical Engineering, Washington University in St. Louis, 1 Brookings Drive, St. Louis, MO 63130. brentw@wustl.edu.

1 | INTRODUCTION

Although people in developed nations spend up to 90% of their time indoors,^{1,2} the chemistry and composition of indoor air remain understudied, especially compared to the outdoor environment.³ Evaluating air quality in residential dwellings is particularly important for several reasons. First, although building standards (eg, for minimum air change rates and moisture control) have been established over the past several decades,^{4,5} many residential structures fail to meet these standards, especially older buildings. Newer buildings, designed to minimize outdoor-to-indoor infiltration for improved energy efficiency, often have higher concentrations of airborne pollutants that are released indoors from materials and activities.^{6,7} Concentrations and composition of indoor particles and gases are influenced by common human activities such as food cooking⁸⁻¹⁶ and cleaning.¹⁷⁻²⁴ As in outdoor air, some directly emitted “primary” gas-phase pollutants can undergo oxidation to produce “secondary” pollutants, which partition to the particle phase to form secondary organic aerosol (SOA), as commonly occurs when gas-phase terpene molecules (eg, limonene and α -pinene) from cleaning products and air fresheners react with ozone (O₃).²⁵⁻²⁹

Recent research has advanced understanding of how infiltrating outdoor-originating pollutants influence the indoor environment.³⁰⁻³⁴ For example, in their investigation of outdoor-to-indoor particle transport within a multi-use building, Johnson et al³² found that for several aerosol particulate components, including black carbon, nitrates, sulfates, and organic aerosol (OA), particulate infiltration is affected by variables including the indoor-to-outdoor temperature gradient and relative humidity. However, the impact of these variables in a home with natural ventilation (eg, window opening and closing to regulate indoor temperature) is not well-characterized.

Natural ventilation is increasingly promoted as an environmentally and economically sustainable practice to meet home cooling requirements, particularly as a warming global climate drives higher outdoor temperatures.^{35,36} From their visual survey, Johnson and Long³⁷ report that frequent household window/door opening (>35% of surveyed instances) was associated with low land area, low population density, and economic status below the poverty line. Morrison and Date³⁸ observed that averaged over all seasons, 46% of homes nationwide had at least one window open on a given day. In addition to increasing outdoor pollutant transport indoors by increasing air exchange rates (AER), natural ventilation causes changes in temperature, pressure, humidity, and gas/particle concentrations inside the home that alter the phase partitioning of semivolatile and intermediately volatile organic compounds (SVOCs and IVOCs, respectively). Many indoor-originating pollutants, including phthalates and aldehydes, are classified as S/IVOCs and partition at relevant time scales between the gas and particle phases depending on temperature, pressure, and particulate matter (PM) concentrations.³⁹ Because respiratory deposition is dependent on chemical and physical properties such as diffusivity,⁴⁰ particle aerodynamic diameter,^{40,41} and particle hygroscopicity,⁴²⁻⁴⁴ greater understanding of pollutant phase partitioning is needed to improve inhabitant toxicant exposure estimates.

To investigate the influence of natural ventilation on indoor air quality in a residential dwelling, we conducted the air composition and reactivity from outdoor and indoor mixing (ACRONIM) study at a single-family residence in urban St. Louis, Missouri, USA. Our goal was to measure a wide range of gas- and particle-phase contaminants inside and outside a residence and to determine how increasing natural ventilation influences the composition of these pollutants. The ACRONIM study was conducted with four major sampling conditions over which we varied home occupancy and the extent of natural ventilation by opening windows. In this work, we present data from the first three sampling periods wherein the home was unoccupied.

2 | MATERIALS AND METHODS

In this study, a suite of instruments obtained chemical and physical measurements of particles and gases both inside and outside the home. Among the instruments deployed was a thermal desorption aerosol gas chromatograph (TAG), which provided hourly in situ chemically speciated measurements of particles and gases in the SVOC and IVOC volatility ranges.^{45,46} In addition to the TAG system, volatile organic compound (VOC) adsorbent tubes collected higher-volatility gases that were subsequently quantified offline using gas chromatography-mass spectrometry (GC-MS) and high-performance liquid chromatography (HPLC). Other instruments deployed include gas monitors for O₃ and nitrogen oxides (NO_x), a scanning mobility particle sizer (SMPS) for particle size distributions, and an optical particle counter (OPC) for size distribution measurements of larger particles.

Gas- and particle-phase compounds were identified and quantified, and positive matrix factorization (PMF), a common statistical data analysis tool for outdoor measurements,^{47–52} was applied to key contaminants to determine the extent of covariance of chemical species throughout the study period. Results of this method reveal trends in compound concentrations as the degree of natural ventilation in the home is varied, providing insight into potential indoor contaminant sources as well as physical and chemical processes affecting concentrations of these contaminants in the home.

2.1 | Field site and measurement strategy

The ACRONIM field campaign took place at a single-family residence in urban St. Louis, MO, USA. The home is located approximately 0.5 km south of US Interstate 44 and 2 km west of US Interstate 55 (Section S1, Figure S1). In addition to nearby highways, potential sources of background outdoor OA include regional power plants and local industry, railroad traffic, and biogenic OA originating from photochemically aged isoprene and monoterpenes emitted largely from forested regions to the southwest of St. Louis.^{53,54}

The study lasted from July 22 to August 4, 2016 and was divided into four sampling periods:

1. Windows Closed (WC; 7/22/16 22:00–7/29/16 14:00): The test home was closed to the outdoor environment. The first VOC adsorbent tube was collected starting 7/22/16 at 22:00, and other instruments began sampling subsequently as they became available.

2. One Window Opened (1WO; 7/29/16 14:00–7/31/16 10:00): One window was opened on the southeast side of the home.
3. Two Windows Opened (2WO; 7/31/16 10:00–8/1/16 18:00): The southeast window remained open, and an additional window was opened on the northeast side of the home.
4. Home Occupied (8/1/16 18:00–8/4/16 10:00): Researchers occupied the residence and performed typical household tasks (eg, cooking and cleaning). Results from this sampling period are not presented in this manuscript and will be addressed in future publications.

The test home was unoccupied during the first three sampling periods. All doors and windows (other than those opened during the 1WO and 2WO sampling periods; Section S1, Figure S2) were closed. The home consists of a basement, a ground floor, and an upstairs level. The basement doorway was sealed off during the study and is not considered part of the home HVAC volume (ie, no air vents or returns located in the basement). Air conditioning (AC) was on to regulate temperatures inside the home and cycled approximately every hour throughout the study period. The AC circulates indoor air using a blower and passes through a filter that was installed new at the start of the study. Air duct vents are located in each room, and the main air return on the measurement floor is located in the home's kitchen. A floorplan for the sampling floors of the home is provided in Figure S2, Section S1.

Hexafluorobenzene (HFB) and octafluorotoluene (OFT) tracer gases were placed in an upstairs bedroom and in the living room, respectively, and continuously emitted through a fixed diffusion tube throughout the study period. Tracer gas concentrations were measured by offline gas chromatography-mass spectrometry (GC-MS) analysis of gas adsorbent tubes collected through inlets located in the instrument trailer (see Figure S2). Air exchange rate was determined as follows:

$$\text{AER}(\text{h}^{-1}) = \frac{E_{\text{Tracer}}}{V \times C_{\text{Tracer}}} \quad (1)$$

where E_{Tracer} is the known tracer emission rate ($0.48 \mu\text{g h}^{-1}$ for HFB, $0.28 \mu\text{g h}^{-1}$ for OFT), V is the volume of the home (509 m^3), and C_{Tracer} is the tracer concentration ($\mu\text{g m}^{-3}$). Because HFB was not reliably calibrated for mass during GC-MS analysis, AER is reported in h^{-1} for OFT only. However, because signal-to-noise ratios were higher for HFB than for OFT, and because the HFB integrated abundances obtained here are typically in the linear dynamic range for this GC-MS method, HFB raw integrated abundances are used to evaluate trends in AER in subsequent analysis and discussion. Furthermore, because the emitters were placed on separate floors, the similarity between trends in inverted raw integrated HFB abundances and OFT-derived AERs illustrates that the house is well mixed until the second window is opened (Figure S3).

A diagram of the experimental setup is provided in Figure 1. Indoor sample line inlets were installed at the center of a first-floor room on the southwest side of the house, inside a window that was otherwise sealed (see Figure S2). Outdoor sample line inlets were installed

on the roof of the house, approximately 6 m above the ground. Cyclones were installed at each particle sample line inlet and provided a particle cutoff (d_{p50}) of approximately 2.2 μm under typical flow rates of 18.5 L min^{-1} . A subset of instruments sampled on an indoor/outdoor switching schedule between two insulated 7.6 m \times 1.27 cm inner-diameter (i.d.) copper lines. Indoor/outdoor sample switching was achieved using two ball valves, which directed flow alternately through the outdoor and indoor sample lines with 2-hour time resolution. Instruments on this switching schedule sampled through 0.952 cm i.d. and 0.635 cm i.d. copper lines down-stream of the ball valves. All instruments on this schedule sampled continuously through either the indoor or outdoor sample line with the exception of the TAG, which only sampled for 30 minutes every hour and drew flow through a built-in bypass line when not sampling to maintain constant total flow through the main inlet. Because active flow was not maintained through non-sampling lines, data collected within 5 minutes of a valve switch are discarded.

2.2 | Instrumentation

Figure 2 illustrates the sampling schedule over a typical 4-hour period, and Table 1 provides a list of instruments with their respective measurement, sampling resolution, and location. Particle size distributions were measured alternately indoors and outdoors using a scanning mobility particle sizer (SMPS; Model 3081 DMA, Model 3022A CPC, TSI, Inc). In this work, we report SMPS data as mass concentrations for particles with diameters within 14–673 nm, assuming spherical particles and a density of 1.2 g cm^{-3} . An indoor PM optical particle counter (Lasair II Mobile Particle Counter, Model 510, Particle Measuring Systems), which sampled aerosol inside the bedroom of the home (same location as main inlet lines), complemented indoor particle concentration measurements obtained with the SMPS, and extended to larger particle sizes, although only for a few wide-range size bins (Figure S4). An aethalometer (AE33, Magee Scientific) measured aerosol light absorption at seven wave-lengths spanning the near ultraviolet to near infrared spectrum (370–1050 nm); however, indoor measurements were below the detection limit for most of the study and are therefore not reported in this work. Nitrogen oxide (NO_x) concentrations were obtained using a trace-level $\text{NO-NO}_2\text{-NO}_x$ analyzer (Model 42i-TL, Thermo Fisher Scientific; data provided in Figure S5). Indoor and outdoor O_3 concentrations were measured simultaneously using separate inter-calibrated O_3 monitors (Indoor: Model 211, Outdoor: Model 202, 2B Technologies). Temperature and relative humidity (RH) sensors (Davis instruments Vantage Pro2, Sensor model 6382) recorded outdoor and indoor RH and temperature throughout the study period (Figure S6). While temperature gradient effects on indoor species are evaluated in subsequent discussion, RH gradient effects are not examined in this work, as RH primarily affects gas-to-particle partitioning of water-soluble compounds^{32,55,56} which were not evaluated in detail using TAG or VOC chemical data. Previous work has demonstrated that lower indoor RH relative to outdoor RH will result in a loss of particle mass as water-soluble species within infiltrating particles increasingly partition to the gas-phase.³²

Volatile organic compound adsorbent tubes sampled organic gases simultaneously indoors and outdoors throughout the study period. Standard stainless-steel adsorbent tubes (Markes International, Inc) were packed with 300 mg of Tenax-TA (Sigma-Aldrich) and

conditioned prior to sample collection. Adsorbent tubes were calibrated by adding known amounts of analytical standards to the sorbent and analyzing by thermal desorption-gas chromatography-mass spectrometry (TD-GC-MS) as described in Section S3.

Two separate polytetrafluoroethylene (PTFE) sample lines were deployed for VOC transfer, with one inlet located outside and one inside at locations described in Section S1 (Figure S2). Each sample line pulled at a flow rate of 10 L min⁻¹. An automated sampling system was used to take adsorbent tube samples from the two air streams separately and simultaneously, switching to new sampling tubes every 4 hours. Sub-samples from the main flow were drawn through each adsorbent tube at ~0.02 L min⁻¹ for 4 hours for a total of approximately 4.8 L (actual flow rates were recorded for each sample). After sampling, sorbent tubes were capped, sealed in aluminum foil, and stored temporarily in portable coolers with cold packs. Within 24 hours, they were transferred to a refrigerator until analyzed. All sample tubes were pre-labeled with sequential numbers, which were logged along with flow rates, date, time, and sample location.

The TAG sampled aerosol on the indoor/outdoor switching schedule, collecting for 30 minutes every hour at typical flow rates of 15 L min⁻¹. Although the TAG was designed for particle measurements, previous studies have demonstrated that the TAG can collect semi- and intermediately volatile gases via diffusion to the collection cell's interior walls.^{46,57} To assess relative contributions of collected gases and particles, the TAG sampled alternately through a parallel-plate carbon denuder (Sunset Laboratory, Inc) and a 0.952 cm i.d. copper bypass line. Switching between the denuder and bypass line was achieved using an automated three-way ball valve (Swagelok Company). This sampling schedule allowed collection of a denuded (particles only) and a non-denuded (particles and gases) sample for each 2-hour indoor or outdoor sampling period. We note that with this version of the TAG collection cell, the collection efficiency of the gas fraction of the SVOC and IVOC molecules becomes less efficient as the phase partitioning begins to favor the gas-phase.⁴⁶ The approximated particle fractions (f_p) reported here become less accurate (and represent an upper limit of f_p) as values go below 0.5 and are dominantly present in the gas-phase. However, relative changes across window-opening conditions can still be informative on the direction of phase equilibrium changes, and we therefore report the observed values in Section 3.

The TAG's sample collection and analysis methodology have been described in previous work.^{45,54} Briefly, aerosol is collected through an inertial impactor onto the surface of a custom collection and thermal desorption (CTD) cell. Following collection, the sample is thermally desorbed at 310°C over a helium stream, through a heated transfer line (310°C), and onto a GC column held at 40°C, where the sample recondenses. Within the GC (Model 6890, Agilent Technologies), the recondensed material is separated through a 30 m × 0.25 mm i.d. capillary GC Rxi-5Sil MS column with a non-polar 0.25-μm-thick stationary phase (Restek Corporation). An electron ionization quadrupole mass spectrometer (Model 5973, Agilent Technologies) serves as the detector and scans over the ion range 29–450 m/z . Instrument performance was evaluated regularly using a C₁₀-C₄₀ even alkane standard (Sigma-Aldrich) as well as a multi-component standard that included deuterated alkanes, polycyclic aromatic hydrocarbons (PAHs), alcohols, aldehydes, monoterpenes, and various

other compounds (Section S4 and Table S1). Standard solutions were injected as liquids onto the surface of the CTD cell using the injection port developed by Kreisberg et al.⁵⁸

During sample thermal desorption, the CTD cell is ramped at 50°C min⁻¹ over a helium carrier stream. While some material volatilizes during desorption, a fraction of the collected sample is too thermally labile to successfully volatilize and instead decomposes into smaller gas-phase fragments, which elute between minutes 6 and 16 of analysis in the thermal decomposition period of the chromatogram (Figure 3).⁵⁴ In this study, the TAG thermal decomposition period was used to evaluate indoor infiltration of outdoor particles using two outdoor-originating species: sulfates (*m/z* 64) and isoprene epoxydiol-derived SOA (IEPOX SOA, *m/z* 82). Since sulfate aerosol has few indoor sources, is minimally reactive, and exhibits low volatility,⁵⁹ it has been used in previous indoor air quality studies as a tracer for infiltrating outdoor aerosol.³² Similarly, IEPOX SOA is a suitable tracer for infiltrating outdoor aerosol because it has a well-characterized regional source^{60–63} and has been measured in ambient collections in the St. Louis area.^{54,63} Data from previous field work demonstrate that for both fragment ions, the TAG decomposition signal agrees well with ions measured by an AMS.⁵⁴

2.3 | Data analysis

Adsorbent tubes were analyzed by thermal desorption followed by TD-GC-MS (analysis details provided in Section S3). Thermal desorption aerosol gas chromatograph compounds were identified using the National Institute for Standards and Technology (NIST) MS search program version 2.0g, available for download at chemdata. nist.gov/mass-spc/ms-search/. The Palisade complete mass spectral library (600K edition, Palisade Mass Spectrometry) was also used to supplement compound identification. Compounds are reported with varying degrees of certainty according to the following criteria: (A) The compound was positively identified using standard injections; (B) the compound was identified with a match quality above 75% using mass spectral libraries; and (C) the compound was identified with a low-to-moderate match quality, between 25% and 75%, using mass spectral libraries. Compound identifications and integrations were facilitated by the TAG ExploRer and iNtegration package software (TERN, version 2.1.10),⁶⁴ written for Igor Pro (version 6.38B01, Wavemetrics, Inc). Integrations were performed on a single ion for each compound and reported as relative ion signal abundance, and in some cases, the multi-peak fitting package (MPF2, built into Igor Pro) enabled integration of co-eluting peaks.

Positive matrix factorization is a widely utilized tool to determine groupings of covarying components. For atmospheric studies, it has been used to separate input gas or particle chemical components into covarying groups (or factors). Individual factors are typically interpreted as representations of specific sources or transformative processes within the context of other supporting data and information. In this study, PMF calculations were performed on a subset of integrated TAG compounds to evaluate major groupings of compounds that could be associated with similar sources or transformation processes. Species included in PMF analyses were chosen to span a variety of volatilities and compound classes across the full GC retention time range. Additionally, to capture broad trends driven by gradual window opening rather than short-timescale emission events, we

only included compounds present in 30% of chromatograms or more across the study period.

Positive matrix factorization calculations were performed separately on peak abundances from denuded (particles) and non-denuded (particles and gases) chromatograms and in both cases included both indoor and outdoor samples. For each case, a compound integration matrix with m rows (number of chromatograms/samples, each with a corresponding collection time) and n columns (number of compounds) and a corresponding $m \times n$ error matrix were supplied to the PMF2 algorithm.⁴⁷ PMF results were evaluated and post-processed using the PMF Evaluation Tool version 3.00A developed for Igor Pro.⁴⁹ To illustrate basic trends that occur with natural ventilation, we present a simple three-factor solution for both denuded and non-denuded data. Positive matrix factorization analysis details, including a description of error calculation methods, pre-processing methods, residuals, and other relevant calculated parameters, are provided in Section S6, Figures S7–S10 and Tables S3–S5. A similar PMF analysis was performed separately on adsorbent tube VOC species and is evaluated along with the two previously described TAG PMF analyses.

3 | RESULTS AND DISCUSSION

3.1 | Windows closed

Example TAG chromatograms for each sampling condition, taken during the WC period, are displayed in Figure 3. A full compound list is provided in Table S2 (Section S5). From indoor and outdoor chromatograms across the study period, 206 individual compounds were identified with mid- to high certainty (identification confidence of “C” or above). As demonstrated in Figure 3, non-denuded chromatograms collected indoors exhibit high overall abundances compared to denuded chromatograms collected either indoors or outdoors, indicating large gas-phase fractions of SVOCs and IVOCs indoors. Within the indoor chromatograms, total compound-period integrated signals in non-denuded chromatograms exceed those in denuded chromatograms by a factor of approximately 3 during the WC sampling period (Section S7, Figure S11).

Indoor compounds, prior to window opening, are dominated by plasticizers (eg, phthalates) and personal care product additives (eg, isopropyl myristate and various siloxanes). The two compounds with the highest peak abundances across all indoor chromatograms are diethyl phthalate and trimethyl pentanyl diisobutyrate (trade name TXIB, Eastman Chemical), which coelute at minute 29, but are distinguishable through distinct mass spectra. Shields et al⁶⁵ report both compounds in the indoor atmosphere of commercial buildings with varying occupant densities. In their study, TXIB, a plasticizer often used in vinyl products (eg, floor and wall coverings, hand tools), was detected in particles in over 50% of commercial buildings surveyed.⁶⁵ Other plasticizers measured in indoor and outdoor chromatograms include several phthalate esters (dimethyl phthalate, diethyl phthalate, dibutyl phthalate, and others), which are commonly measured in indoor particles and gases,^{65–69} and 2-ethylhexyl benzoate, a monobenzoate that has been reported as an additive to nitrile rubber⁷⁰ as well as an ingredient in cosmetics and fragrances.^{71,72}

High indoor gas concentrations relative to outdoor gas concentrations were also observed in VOC adsorbent tube data. Individual compound concentrations (\pm one standard deviation) for selected compounds are provided in Table S6 (Section S8). Prior to window opening, indoor VOCs were dominated by aldehydes and ketones, most significantly formaldehyde, acetaldehyde, and acetone, with average concentrations of 10.4 ± 2 ppb, 11.7 ± 4 ppb, and 78.5 ± 20 ppb, respectively. Aldehydes are common indoor pollutants that originate primarily from building products and human activity (eg, combustion from food cooking and tobacco smoking).^{73,74} Specifically, formaldehyde is commonly emitted from wooden furniture and flooring, as well as some fabrics.⁷⁵ Typical indoor formaldehyde concentrations range from 20 to 60 $\mu\text{g m}^{-3}$, two to six times as high as those observed in this unoccupied home study.⁷³ Acetaldehyde is emitted from construction lumber and as a by-product of incomplete combustion from food-cooking,⁷⁴ and previously reported indoor concentrations range from 10.5 to 60 ppb.^{73,76,77} Although formaldehyde and acetaldehyde are often observed as by-products of cigarette smoking,⁷⁸ no contribution from smoking is expected in the non-smoking test home. Acetone, which may originate indoors from a variety of sources including cleaning products and nail polish remover,^{79–81} exhibits the highest average concentration of any single VOC species quantified in the home. A wide range of indoor acetone concentrations have been reported in previous literature. For example, Shah and Singh⁸² report typical indoor concentrations of 8 ppb, and Weisel et al⁸³ report an average concentration of 87 $\mu\text{g m}^{-3}$ (approx. 87 ppb) over a range of <12–2900 $\mu\text{g m}^{-3}$, with the highest concentrations occurring in urban rather than rural homes.

Other VOCs measured in significant concentrations inside the home include monoterpenes (eg, limonene, α -pinene, β -pinene, γ -terpinene), oxidized monoterpenes (eg, fenchyl alcohol, camphor, α -terpineol), siloxanes (eg, hexamethyl siloxane, octamethyl siloxane, decamethyl siloxane), aromatic hydrocarbons (eg, benzene, toluene, naphthalene), and alkanes (eg, methylcyclohexane, ethylcyclohexane, undecane). Monoterpenes and oxidized monoterpenes are common indoor contaminants originating from cleaning supplies,^{17,18,21,22,84} and siloxanes are ubiquitous in cosmetics and personal care products.^{85–90} Benzene, toluene, ethylbenzene, and xylene (BTEX) result from fossil fuel combustion and often originate outdoors. However, known indoor sources include building materials, paints, and cleaning products.^{13,91–93} Similarly, infiltrating fuel combustion products may also contribute to indoor alkane concentrations,^{94–96} but alkanes can also originate from materials common indoors.¹³

3.2 | Natural ventilation impacts

To assess the impact of increased natural ventilation on different compounds, and to elucidate various sources and chemical and physical processes affecting components in the home's indoor air, we use PMF to group compounds that covary over time. In Figures 4–7, we explore these trends by averaging indoor chromatogram factor abundances (I) over each of the three natural ventilation conditions, then dividing each average by the average obtained at the windows closed condition (I_{WC}). At the windows closed condition, this normalization results in a ratio (I/I_{WC}) of 1, and an increase or decrease in I/I_{WC} in the window-opened conditions represents the fractional enhancement or depletion (respectively) of that component within the indoor air. Error bars for I/I_{WC} values were obtained by

propagating the standard deviations in integrated abundances across the I/I_{WC} calculations. I/I_{WC} values for each compound included in PMF analyses are provided for TAG and VOC compounds in Tables S7 and S9 (Section S9).

Positive matrix factorization results from calculations on both denuded (particles only) and non-denuded (particles and gases) TAG chromatograms are displayed in Figures 4 and 5, respectively, with calculation details provided in Section S6. In each figure, time series are given in panel A, I/I_{WC} in panel B, and fractional factor loadings for each included compound in panel C (tabulated in Tables S3 and S4). In both denuded and non-denuded analyses, a three-factor solution provided one factor associated with indoor-originating compounds (Factors 2-ND and 2-D) and one associated with compounds undergoing significant enhancements in emission, formation, or infiltration rates following window opening (Factors 1-ND and 1-D). We also obtain a less abundant factor into which outdoor-to-indoor infiltrating components load (Factors 3-ND and 3-D). The abundance of these outdoor-originating species may be influenced by recent infiltration as well as by equilibrium phase partitioning from indoor reservoirs of deposited material which had previously infiltrated from outdoors.

Positive matrix factorization was similarly performed on 30 integrated compounds from outdoor and indoor VOC adsorbent tube collections. We chose a two-factor solution to group covarying VOCs, with Factor 2-VOC-ST corresponding to indoor-originating compounds experiencing depletion with window opening, and Factor 1-VOC-ST encompassing compounds that undergo less depletion. Though in general, we observe higher VOC concentration indoors than outdoors, many of the compounds loading into Factor 1 have both outdoor and indoor sources, (eg, o- and p-xylene, decanal).^{93,97,98} We provide factor time series and I/I_{WC} over the three natural ventilation conditions in Figure 6.

From TAG and VOC adsorbent tube PMF results, we selected several key compounds to illustrate chemical and physical processes occurring as natural ventilation is increased. Individual raw abundance time series for each selected compound are provided Section S7, Figures S12 and S13. Figure 7 displays indoor trends in select TAG and VOC adsorbent tube compounds as I/I_{WC} across three natural ventilation conditions observed in particles (denuded; 7A); approximate particle-phase fraction (f_p), estimated as the ratio of denuded (particles) to non-denuded (particles + gases) averages at each condition (7B); gases (from VOCs and approximate TAG f_g ; 7C); and gases corrected for dilution at each window-opening period by normalizing each I/I_{WC} to the corresponding HFB I/I_{WC} (7D). Although VOC adsorbent tubes sampled with windows closed starting on 7/22/2016, this figure only incorporates VOC WC data obtained while the TAG was online (ie, starting on 7/27/2016) to maximize comparability between TAG and VOC adsorbent tube data. The TAG gas-phase component (7C) was approximated as non-denuded (particles and gases) minus denuded (particle) abundances at each natural ventilation condition. Raw abundances for displayed TAG- and adsorbent tube-measured species are provided in Section S7 (Figures S12 and S13, respectively). In general, compounds displayed in Figure 7 are grouped according to trend with window opening. For example, gases primarily affected by dilution decrease in abundance with window opening but have I/I_{WC} values similar to HFB (Figure 7D). Species that undergo enhanced gas-phase emissions and oxidative formation exhibit I/I_{WC}

values that increase across the two window-opened periods (Figure 7C,D), and increased gas-to-particle partitioning is reflected in increased particle-phase I/I_{WC} and f_p (Figure 7A,B). Limonene and α -pinene, which are expected to react with O_3 indoors, are not significantly depleted beyond dilution, which is reflected in HFB-normalized I/I_{WC} (Figure 7D). Finally, outdoor-originating compounds exhibit consistent I/I_{WC} values in both the particle and gas-phases across the window-opening periods (Figure 7A,C), demonstrating that these species rapidly partition when entering the indoor environment.

To evaluate the impact of outdoor-to-indoor transport of TAG- and adsorbent tube-measured species, indoor-to-outdoor abundance ratios (I/O) for each compound at each natural ventilation condition are provided in Tables S8 and S9, respectively. This outdoor normalization strategy has been used to evaluate net changes in indoor species concentrations as a result of outdoor species infiltration.^{32,99–104} Although this metric has limited utility for pollutants existing predominantly indoors,¹⁰⁵ I/O is helpful for understanding trends in compounds with significant concentrations in both the indoor and outdoor environments. As demonstrated in previous work, changes in species abundance due to mechanisms other than mechanical losses (eg, particle deposition and filtration) can be evaluated by normalizing species-specific I/O to sulfate I/O .^{32,104} Sulfate-normalized I/O ratios ($[I/O]_{i/m/z\ 64}$) for different TAG species were obtained for each natural ventilation condition by normalizing average I/O values to average TAG decomposition period $m/z\ 64$ signals. These ratios are given in Table S8.

As with indoor abundances in previous figures, I/O averages at each natural ventilation condition are normalized to I/O at the windows closed condition to display fractional enhancement and depletion for each compound ($[I/O]/[I/O]_{WC}$; Figures 8 and 9). As with I/I_{WC} , standard deviations are obtained from compound integrated abundances over each natural ventilation condition, propagated through the calculations, and displayed as error bars. For TAG-measured compounds, we provide these values obtained in denuded and non-denuded chromatograms. Partitioning estimates (ie, f_p and gas-phase approximations) were not attempted for the outdoor components due to high observed temporal variability in compound loadings. From outdoor TAG data obtained in Riverside, CA, Williams et al.⁴⁶ modeled seasonal partitioning behavior as a function of vapor pressure and number of carbons for several compound classes, including alkanes, lactones, and PAHs. Based on these data, each compound displayed in Figure 8 is expected to exhibit a low particle-phase fraction outdoors in the summertime ($f_p < 0.2$), with the exception of γ -nonalactone ($f_p \sim 0.25$) and pyrene ($f_p \sim 0.5$). Therefore, we expect the non-denuded $[I/O]/[I/O]_{WC}$ values to primarily reflect trends in the gas-phase. In general, when outdoor concentrations for a given compound are stable, $[I/O]/[I/O]_{WC}$ trends mirror I/I_{WC} trends (Figure 7). Notable exceptions are discussed individually in subsequent sections.

From trends in these compound abundances, we observe four distinct chemical and physical processes occurring when the AER is increased by window opening: outdoor-to-indoor transport, indoor species dilution, enhanced emission of indoor species, and species formation via oxidation. We also evaluate the potential for oxidative depletion of certain compounds (eg, limonene and α -pinene) that were expected to react with infiltrating ozone. We discuss and present evidence for each of these processes individually.

3.2.1 | Outdoor-to-indoor transport—Measurements from the SMPS, the OPC, and the TAG demonstrate the influence of outdoor particle infiltration on indoor particle concentrations and composition. Figure 10 gives time series for TAG decomposition sulfate (m/z 64; 10A) and IEPOX (m/z 82; 10B), along with SMPS total mass concentrations (for particles with diameters within 14–673 nm, assuming spherical particles and an approximate density of 1.2 g cm^{-3} ; 10C), OPC PM_{10} particle counts (Figure 10D), and O_3 concentrations indoors and outdoors (Figure 10E). Thermal desorption aerosol gas chromatograph decomposition m/z 82 and m/z 64 were corrected for excessive noise caused by detector saturation according to methods outlined in Section S10. We observe minimal gas-phase contributions to both TAG decomposition m/z 82 and m/z 64 (Figure S14) and therefore include non-denuded and denuded chromatograms in the same time traces. A reasonably high correlation is observed between m/z 64 and m/z 82 for outdoor samples ($r^2 = .56$), and an even higher correlation for indoor samples ($r^2 = .72$; Figure S15). Marais et al.¹⁰⁶ observe similar correlations between measured sulfate and IEPOX ambient aerosol, reporting r^2 values of .82 and .52 for ground-level and boundary layer field measurements, respectively. As sulfates increase aqueous aerosol acidity, the epoxide bonds in IEPOX species undergo acid-catalyzed ring opening and subsequently react with sulfate to form organosulfate products.^{60,107–109} In the southeastern United States, these organosulfates contribute as much as half of all IEPOX-derived SOA.^{60,110,111}

In the TAG decomposition and SMPS data, indoor and outdoor measurements converge once windows are opened. Indoor PM_{10} number concentrations measured by the OPC are low throughout the study but do increase by nearly a factor of 3 by the second window-opening period. While outdoor particle mass concentrations (Figure 10C) remain stable during the first window-opened period, they exhibit greater variation after the second window is opened, which is mirrored by indoor concentrations during that time. A depletion in outdoor mass concentrations, as well as TAG IEPOX and sulfate signals, begins around midnight on 8/1/2016 and coincides with a regional rain event occurring between midnight and 7 AM on that day (Figure S6). Previous work has demonstrated that PM_{10} concentrations can be affected by rain washout (though to a lesser extent compared to larger particles),^{112,113} so this event could partially account for the observed depletion in infiltrating particulate species.

Significant changes in indoor O_3 were only measured after the second window opening. A very small increase in ozone may be below the instrument detection limit during the first window-opening period. Alternatively, low observed O_3 concentrations following the first window opening could result from non-uniform mixing in the house. However, as O_3 is rapidly removed indoors by surface reactions,¹¹⁴ some reduction in surface reactivity could occur over time. This reactivity would decrease O_3 surface uptake and increase the ratio of indoor to outdoor ozone concentrations.^{115,116}

Outdoor-originating compounds identified in the TAG and associated with PMF Factors 3-D and 3-ND include PAHs (eg, pyrene, benz[a]anthracene) and heavy alkanes (eg, docosane and pentacosane). In general, outdoor PAH and oxy-PAH (eg, 9H-fluoren-2-one, 9,10-anthracenedione) concentrations are associated with incomplete combustion, particularly from vehicle emissions in urban settings.⁹⁴ Similarly, long-chain alkanes have been

measured in diesel exhaust.^{94–96} Levoglucosenone, a cellulose decomposition product,¹¹⁷ was also observed in TAG chromatograms and has been previously associated with biomass burning aerosol.⁵⁰ Notably, levoglucosan, a less volatile cellulose decomposition product commonly used as a biomass burning tracer,^{118–121} was not observed in any outdoor TAG samples. Outdoor abundances of γ -nonalactone do not have a single clear source, though the compound is used as a coconut-like perfumant¹⁰² and has been observed in beer¹²² and American whiskey¹²³ as a by-product of fermentation.^{124,125} Ramalho et al¹²⁶ have reported airborne alkyl lactones as products of cellulose degradation in building materials.

Based on TAG-sulfate-normalized *I/O* ratios (Figure 8 and Table S8), several particle-phase compounds loading primarily into Factor 3-D, including 9,10-anthracenedione, 1,4-dimethylantracene, and tetracosane, exhibit increases in indoor abundances consistent with outdoor-to-indoor infiltration. However, for other compounds loading into factors 3-D and 3-ND, variations in indoor abundances with natural ventilation are more complex. While indoor and outdoor S/IVOCs will ultimately equilibrate over long time scales, short-term phase partitioning dynamics depend on relative fugacities between phases indoors and outdoors, as well as indoor-to-outdoor differences in RH and temperature. As displayed in Figure 7A,C, *I/I_{WC}* for pyrene and γ -nonalactone remains relatively stable in the particle and non-dilution-normalized gas-phases with window opening, consistent with relatively fast equilibration between outdoor and indoor concentrations. In addition, indoor surfaces play a key role in the equilibration of outdoor-originating S/IVOCs in the indoor environment. Over time, infiltrating particles and gases will partition to these surfaces, resulting in a reservoir of these compounds in organic surface films. Subsequently, whenever natural ventilation is increased, S/IVOCs in the particle phase will equilibrate rapidly with the indoor environment (gases, particles, and surfaces), resulting in stable indoor gas-phase concentrations. For example, increased gas-phase γ -nonalactone after the first window opening (Figure S12), reflected in a net increase in $[I/O]/[I/O]_{WC}$ (Figure 8), could result from surface-to-gas partitioning as previously deposited material equilibrates with infiltrating γ -nonalactone in the particle phase. Since most compounds measured by the TAG in this study are S/IVOCs (Table S2), we expect a combination of these factors to drive changes in indoor abundances with natural ventilation.

3.2.2 | Dilution of indoor species—Following window opening, several gas-phase species were depleted at the same rate as the gas-phase tracers, indicating that indoor concentrations are primarily affected by dilution for these compounds. These species include methylcyclohexane, emitted indoors by glues, paints, and other materials,¹²⁷ and cosmetic component cyclopentasiloxane (D5 siloxane).^{85–90}

From TAG PMF results, we observe a similar trend in both Factors 2-D and 2-ND (Figures 4 and 5, respectively) with window opening, which comprises many of the TAG-measured indoor-originating solvents, plasticizers, and personal care product components. Among the key TAG-measured components examined in Figure 7, the gas fraction of pentadecane, tetradecamethylhexasiloxane, and D7 siloxane exhibits the greatest decrease with window opening (Figure 7C), though do not appear to decrease as much as the indoor gas-phase tracers (Figure 7D). If these compounds are emitted entirely from indoor sources, this trend, when considered along with particle-phase depletion of these species (Figure 7A),

could indicate partitioning from the particle to the gas-phase with changing concentration gradients inside the home. Additionally, altered convection patterns could drive increased deposition of particles, contributing to net particle-phase depletion of these compounds.

3.2.3 | Enhanced emission of indoor species—Notably, several compounds originating indoors exhibited enhancement following window opening despite significant dilution. From non-denuded TAG PMF results (Figure 5), Factor 1-ND displays this trend with window opening, where some compounds are enhanced only indoors (not outdoors) when the windows open. Factor 1-D from particle-phase PMF results exhibits this trend as well (Figure 4), reflecting gas-to-particle partitioning of these species as windows are opened. Though relative factor loadings may vary between denuded and non-denuded measurements for a given compound, Factors 1-D and 2-D generally have contributions from personal care product ingredients (eg, isopropyl myristate¹²⁸ and DEET¹²⁹), perfumes (eg, hedione¹³⁰ and α -cedrene¹³¹), and plasticizers (eg, diethyl phthalate, dibutyl phthalate, and dimethyl phthalate loading into both indoor factors 1 and 2).^{65–69} Carvone, which was primarily observed in non-denuded indoor chromatograms, is an oxidized terpene that, like other terpenes, emits as a primary product from wood, paints, and scented indoor items, but also originates from gas-phase oxidation of limonene.^{132,133} Although the limonene-ozone pathway might contribute partly to carvone concentrations, we do not expect significant carvone production through this mechanism based on low observed limonene concentrations.

As particle outdoor-to-indoor infiltration rates increase with window opening, S/IVOCs abundant in the gas-phase are expected to partition to the increased surface area provided by infiltrating particles. This trend is reflected in Figure 7A,B, which displays increases in particle-phase S/IVOC abundances and f_p values across the three window-opening conditions. Temperature gradients from outdoors to indoors are also expected to influence S/IVOC phase partitioning: Positive temperature gradient with respect to the indoor environment (ie, indoor temperatures are lower than outdoor temperatures) will further drive S/IVOCs to the condensed phase, while a negative gradient will promote partitioning of S/IVOCs into the gas-phase. Because the temperature gradient exhibits a diurnal trend (Figure S6), temperature-driven gas-to-particle partitioning is expected to vary diurnally as well. However, we predict that temperature gradient effects are small with respect to gas-to-particle partitioning driven by increasing particle mass concentrations (Section S11).

To further evaluate the impact of gas-phase S/IVOC condensation onto infiltrating outdoor particles, I/I_{WC} for the particle-only fraction of several compounds loading into Factors 1-D and 2-D (enhanced and indoor factors, respectively; Figure 4) were normalized to the TAG's decomposition m/z 64 I/I_{WC} (Section S12 and Figure S18), which serves as a chemical tracer for infiltrating outdoor aerosol (Figure 10B). Compounds loading into the indoor-originating Factor 2 (pentadecane, tetradecamethylhexasiloxane, D7 siloxane, α -cedrene) are still depleted across the window-opening conditions following normalization to TAG-measured sulfate, indicating they experience more significant dilution in the gas-phase and/or less significant gas-to-particle partitioning with window opening. Sulfate-normalized TXIB, which loads primarily into Factor 2-D, yet loads significantly into Factor 1-D, is depleted to a lesser extent. By contrast, compounds that remain consistent or even exhibit

enhancement across the three natural ventilation conditions after sulfate normalization include isopropyl myristate, DEET, and diethyl phthalate, all of which load primarily into Factor 1 (the indoor enhancement factor). Increased partitioning to infiltrating particles with window opening, in conjunction with enhanced indoor gas-phase emission rates, would account for the trends observed in these compounds across the study period.

As shown in Figure 7C,D, we observe enhancements in certain contaminants in both TAG and VOC adsorbent tube data that are not attributed to outdoor infiltration. Previous studies have shown that for certain gas-phase indoor pollutants, including naphthalene¹³⁴ and phthalates,^{135,136} depletion rates do not match enhanced ventilation rates if dilution alone is considered.^{126,127} This discrepancy can be attributed in part to enhanced species partitioning from surface films to the gas-phase, which is driven by changes to gas-phase concentration gradients at the surface boundary layer.^{135,137,138} Additionally, in a competing effect, increased AERs can promote higher near-surface air velocities, which increase gas-to-surface mass transfer coefficients and therefore drive gas-phase pollutant concentrations down.^{138–140} The data obtained in this study reflect a strong enhancement effect for many gas-phase pollutants, particularly for S/IVOCs measured with the TAG. Therefore, for these compounds, we expect that increases in vertical concentration gradients with increased AER are the predominant drivers for changes in emission rates.

Although the average AER was similar for the two window-opening conditions (Figure S3), the dilution of the tracers emitted upstairs (HFB) and downstairs (OFT) differed more with two windows open. This suggests that opening the second window resulted in poorer whole-house mixing and altered the direction of airflow through the house, affecting different surfaces with different organic film compositions and thicknesses. Thus, the enhancements observed in compounds loading into PMF Factors 1-ND and 1-D are not entirely due to changes in AER. Additionally, enhancement effects are dependent on the compound's volatility. A volatile compound partitioning predominantly into the gas-phase is more likely to remain in the gas-phase and will therefore be strongly affected by dilution and other gas-phase processes. By contrast, compounds in the S/IVOC volatility range will instead partition partly to indoor surfaces, resulting in the development of a surface film reservoir; when windows are opened and gas-phase compound concentrations are depleted close to the surface films, compounds from the reservoir are driven into the gas-phase, resulting in the observed enhancement. We observe the influence of volatility on enhancement effects in the data. For example, when comparing trends in D5 and D7 siloxanes (two minimally reactive species with similar chemical properties), the less volatile D7 siloxane exhibits an increase with window opening above dilution effects while the more volatile D5 siloxane does not. When considered in the context of previous work, our results suggest that window opening drives multiple concurring phase partitioning effects, each of which impacts overall indoor gas-phase pollutant concentrations depending on indoor environmental characteristics and time scales.¹³⁸

3.2.4 | Formation of indoor species through oxidation—Several compounds produced through indoor oxidation were included in PMF analysis and evaluated across the three natural ventilation conditions. The compounds evaluated for potential secondary origins loaded significantly into Factors 1-D and 1-ND (enhanced) in either or both of the

TAG PMF results (Figures 4 and 5), and based on previous literature, we largely attribute their increase with natural ventilation to enhanced oxidative formation with increased outdoor-to-indoor transport of oxidants, particularly O₃. Figure 7 demonstrates increases in both particle- and gas-phase abundances for nonanal and decanone, two species produced as a result of oxidation processes in the indoor environment.

Nonanal has been studied extensively in the indoor environment and is a product of surface film ozonation. Weschler et al¹⁴¹ determined that several aldehydes (pentanal through decanal) can be produced from ozonation of unsaturated organics on carpeting, suggesting unsaturated fatty acids as potential precursors. Wang and Morrison¹⁴² also found significant nonanal emissions from carpeting, particularly from carpet less than a year old. In addition to carpeting, indoor nonanal is produced from unsaturated fatty acid ozonation mediated by a variety of indoor surfaces.^{116,142} For example, in their field investigation of secondary chemistry in five test homes, Wang and Morrison¹¹⁶ found that nonanal was the most predominant secondary aldehyde produced from any surface, with particularly high emission rates in kitchens, where surface films have significant contributions from cooking oils. In the unoccupied study, we did not observe significant concentrations of unsaturated fatty acids in the gas or particle phases. For this reason, we hypothesize that the increase in indoor nonanal with window opening is coming dominantly from surface reactions with precursors in organic surface films.

Like nonanal, indoor 2-decanone is enhanced in both particle and gas-phases with window opening, potentially due to oxidative chemistry. 2-decanone has been measured in emissions from used (but not new) linoleum floors as a product of degradation reactions.¹⁴³ In their study of gas-phase emissions from carpet, Morrison and Nazaroff¹⁴⁴ report that aliphatic ketones, including 2-decanone, are produced almost exclusively from ozonation of gas-phase primary carpet emissions.

3.2.5 | Depletion of indoor species through oxidation—Limonene and α -pinene are expected to react rapidly with O₃ relative to other common indoor VOCs.¹¹⁴ To evaluate potential oxidative depletion for these two compounds, we examined indoor concentrations and found that when normalized to the indoor gas-phase tracer, they were not depleted beyond statistical significance (Figure 7D).

The lack of observable depletion beyond dilution could occur for several reasons. First, competing processes could contribute to increasing monoterpene concentrations with window opening. For example, limonene and α -pinene could undergo some enhanced emission from surfaces, which might overshadow oxidative depletion at these time scales. Outdoor limonene and α -pinene concentrations could also contribute to increased indoor concentrations through more efficient outdoor-to-indoor transport at higher AERs, though this effect is likely small based on low observed outdoor abundances (Figure S12).

More likely, observations of limonene and α -pinene ozonation are limited by low time resolution and limits of detection. Based on trends in indoor ozone concentrations (Figure 10), these monoterpenes are expected to deplete most rapidly with two windows opened. Additionally, we anticipate a diurnal pattern in depletion rates, since outdoor ozone

concentrations are highest in the mid-afternoon (Figure 10). However, since the two-window-opened unoccupied period was only 32 hours long, and because the adsorbent tubes collected across 4 hours, patterns in oxidative depletion are difficult to identify in these data. Furthermore, we attempted to track monoterpene oxidation products with window opening, but with the exception of carvone (which may be both a primary emission and a limonene oxidation product), we were unable to reliably quantify potential oxidation products across the duration of the study period in either TAG or VOC data. Given that each precursor produces a variety of oxidation products,^{145–149} we expect many products to be below limits of detection for both chemical analysis methods as they were operated here. Despite this limitation, newly developed techniques for analyzing unresolved complex mixtures (UCM) may provide greater insight into trends in compounds and compound classes that would not otherwise be detectable.^{51,52} This improved analysis will be the subject of future publications.

4 | CONCLUSIONS AND IMPACTS

Five distinct chemical and physical processes resulting from changes in indoor natural ventilation were explored using TAG and VOC adsorbent tube measurements taken during the unoccupied period of the ACRONIM field campaign. Simple two- and three-factor PMF solutions, obtained from integrated chromatographic compound abundances across indoor and outdoor collections, allowed for rapid grouping of compounds into covarying factors, facilitating exploration of these processes across three natural ventilation conditions. Although low time resolutions for chemical measurements (4 hours) challenged our investigation of the rapidly changing indoor environment, the in situ collection and molecular-level analysis provided by the TAG improve upon techniques used to investigate indoor OA molecular composition from previous studies.

The findings presented in this work suggest that the overall indoor air quality impacts of natural ventilation depend on multiple factors, including indoor pollutant abundances (eg, high gas-phase S/IVOC abundances due to offgassing of building materials and personal care products), outdoor pollutant abundances (eg, outdoor particle concentrations and composition, O₃ concentrations), and AER. The contributions of each process will therefore vary between buildings and their surrounding environments, necessitating future investigation across a variety of test homes in a variety of locations. Additionally, human occupancy presents additional challenges to assessing natural ventilation impacts on indoor air quality. For example, while opening windows can mitigate indoor pollutant concentrations from activities like food cooking or cleaning, infiltrating O₃ can drive oxidation of these particles and gases to form secondary products, and clothing and skin can drive formation of secondary particles and gases through surface-mediated ozonation.^{3,150,151} The influence of human occupants is therefore critical to understanding natural ventilation impacts on the indoor environment and will therefore be explored in future work.

Supplementary Material

Refer to Web version on PubMed Central for supplementary material.

ACKNOWLEDGEMENTS

This publication was developed under Assistance Agreement No. 83575101 awarded by the US Environmental Protection Agency (EPA). It has not been formally reviewed by the EPA. The views expressed in this document are solely those of the authors and do not necessarily reflect those of the Agency. The EPA does not endorse any products or commercial services mentioned in this publication. The authors would like to thank Jiayu Li for providing the floorplan for the test home.

Funding information

U.S. Environmental Protection Agency, Grant/Award Number: 83575101

REFERENCES

1. Klepeis NE, Nelson WC, Ott WR, et al. The National Human Activity Pattern Survey (NHAPS): a resource for assessing exposure to environmental pollutants. *J Expo Anal Environ Epidemiol*. 2001;11:231–252. [PubMed: 11477521]
2. Leech JA, Nelson WC, Burnett RT, Aaron S, Raizenne ME. It's about time: a comparison of Canadian and American time–activity patterns. *J Expo Sci Environ Epidemiol*. 2002;12:427–432.
3. Morrison G. Recent advances in indoor chemistry. *Curr Sustain Energy Rep*. 2015;2:33–40.
4. US EPA O. Building Codes and Indoor Air Quality. Washington, DC: US EPA. 818, 2014. <https://www.epa.gov/indoor-air-quality-iaq/building-codes-and-indoor-air-quality>. Accessed May 25, 2018.
5. Household Air Pollution and Health. Geneva, Switzerland: World Health Organization. <http://www.who.int/news-room/fact-sheets/detail/household-air-pollution-and-health>. Accessed May 25, 2018.
6. Wargocki P. What are indoor air quality priorities for energy-efficient buildings? *Indoor Built Environ*. 2015;24:579–582.
7. Derbez M, Wyart G, Le Penner E, Ramalho O, Ribéron J, Mandin C. Indoor air quality in energy-efficient dwellings: levels and sources of pollutants. *Indoor Air*. 2018;28:318–338. [PubMed: 28960493]
8. Melia R, Du V, Florey C, Darby SC, Palmes ED, Goldstein BD. Differences in NO₂ levels in kitchens with gas or electric cookers. *Atmospheric Environ*. 1967;1978(12):1379–1381.
9. Lambert WE, Samet JM, Hunt WC, Skipper BJ, Schwab M, Spengler JD. Nitrogen dioxide and respiratory illness in children. Part II: assessment of exposure to nitrogen dioxide. *Res Rep Health Eff Inst*. 1993;58:33–50; discussion 51–80.
10. Jarvis D, Chinn S, Luczynska C, Burney P. Association of respiratory symptoms and lung function in young adults with use of domestic gas appliances. *The Lancet*. 1996;347:426–431.
11. Garrett MH, Hooper MA, Hooper BM, Abramson MJ. Respiratory symptoms in children and indoor exposure to nitrogen dioxide and gas stoves. *Am J Respir Crit Care Med*. 1998;158:891–895. [PubMed: 9731022]
12. Jarvis D, Chinn S, Sterne J, Luczynska C, Burney P. The association of respiratory symptoms and lung function with the use of gas for cooking. European Community Respiratory Health Survey. *Eur Respir J*. 1998;11:651–658. [PubMed: 9596117]
13. Jones AP. Indoor air quality and health. *Atmos Environ*. 1999;33:4535–4564.
14. Evans GJ, Peers A, Sabaliauskas K. Particle dose estimation from frying in residential settings. *Indoor Air*. 2008;18(6):499–510. [PubMed: 19120500]
15. Kim K-H, Pandey SK, Kabir E, Susaya J, Brown R. The modern paradox of unregulated cooking activities and indoor air quality. *J Hazard Mater*. 2011;195:1–10. [PubMed: 21885193]
16. Abdullahi KL, Delgado-Saborit JM, Harrison RM. Emissions and indoor concentrations of particulate matter and its specific chemical components from cooking: a review. *Atmos Environ*. 2013;71:260–294.
17. Weschler C, Shields H. Indoor ozone/terpene reactions as a source of indoor particles. *Atmos Environ*. 1999;33:2301–2312.

18. Wainman T, Zhang J, Weschler CJ, Liyo PJ. Ozone and limonene in indoor air: a source of submicron particle exposure. *Environ Health Perspect.* 2000;108:1139–1145. [PubMed: 11133393]
19. Hodgson AT, Beal D, McIlvaine J. Sources of formaldehyde, other aldehydes and terpenes in a new manufactured house. *Indoor Air.* 2002;12:235–242. [PubMed: 12532755]
20. Lee SC, Li W-M, Ao C-H. Investigation of indoor air quality at residential homes in Hong Kong—case study. *Atmos Environ.* 2002;36:225–237.
21. Sarwar G, Olson DA, Corsi RL, Weschler CJ. Indoor fine particles: the role of terpene emissions from consumer products. *J Air Waste Manag Assoc.* 1995;2004(54):367–377.
22. Destailats H, Lunden MM, Singer BC, et al. Indoor secondary pollutants from household product emissions in the presence of ozone: a bench-scale chamber study. *Environ Sci Technol.* 2006;40:4421–4428. [PubMed: 16903280]
23. Corsi RL, Siegel JA, Chiang C. Particle resuspension during the use of vacuum cleaners on residential carpet. *J Occup Environ Hyg.* 2008;5:232–238. [PubMed: 18247227]
24. Rossignol S, Rio C, Ustache A, et al. The use of a housecleaning product in an indoor environment leading to oxygenated polar compounds and SOA formation: gas and particulate phase chemical characterization. *Atmos Environ.* 2013;75:196–205.
25. Weschler CJ. Ozone's impact on public health: contributions from indoor exposures to ozone and products of ozone-initiated chemistry. *Environ Health Perspect.* 2006;114:1489–1496. [PubMed: 17035131]
26. Waring MS, Siegel JA. Indoor secondary organic aerosol formation initiated from reactions between ozone and surface-sorbed d-limonene. *Environ Sci Technol.* 2013;47:6341–6348. [PubMed: 23724989]
27. Youssefi S, Waring MS. Transient secondary organic aerosol formation from limonene ozonolysis in indoor environments: impacts of air exchange rates and initial concentration ratios. *Environ Sci Technol.* 2014;48:7899–7908. [PubMed: 24940869]
28. Youssefi S, Waring MS. Indoor transient SOA formation from ozone+ α -pinene reactions: impacts of air exchange and initial product concentrations, and comparison to limonene ozonolysis. *Atmos Environ.* 2015;112:106–115.
29. Yang Y, Waring MS. Secondary organic aerosol formation initiated by α -terpineol ozonolysis in indoor air. *Indoor Air.* 2016;26:939–952. [PubMed: 26609907]
30. Rackes A, Waring M. Modeling impacts of dynamic ventilation strategies on indoor air quality of offices in six US cities. *Build Environ.* 2013;60:243–253.
31. Riley WJ, McKone TE, Lai A, Nazaroff WW. Indoor particulate matter of outdoor origin: importance of size-dependent removal mechanisms. *Environ Sci Technol.* 2002;36:200–207. [PubMed: 11831216]
32. Johnson AM, Waring MS, DeCarlo PF. Real-time transformation of outdoor aerosol components upon transport indoors measured with aerosol mass spectrometry. *Indoor Air.* 2017;27:230–240. [PubMed: 27008502]
33. Kearney J, Wallace L, MacNeill M, Héroux M-E, Kindziarski W, Wheeler A. Residential infiltration of fine and ultrafine particles in Edmonton. *Atmos Environ.* 2014;94:793–805.
34. Ji W, Zhao B. Estimating mortality derived from indoor exposure to particles of outdoor origin. *PLoS ONE.* 2015;10(4):e0124238. [PubMed: 25860147]
35. Axley J. Application of Natural Ventilation for U.S. Commercial Buildings Climate Suitability Design Strategies & Methods Modeling Studies. 52018.
36. Natural Ventilation Engineering Guide. Price Industries; 2011. <http://www.pricecriticalcontrols.com/content/uploads/assets/literature/engineering-guides/natural-ventilation-engineering-guide.pdf>. Accessed May 25, 2018.
37. Johnson T, Long T. Determining the frequency of open windows in residences: a pilot study in Durham, North Carolina during varying temperature conditions. *J Expo Anal Environ Epidemiol.* 2005;15:329–349. [PubMed: 15536488]
38. Morrison GC, Date G. Window opening occurrence in the US: influence of climate and region. In: *Proceedings of Indoor Air 2018. Vol Paper 114. International Society of Indoor Air Quality and Climate; 2018.*

39. Donahue NM, Robinson AL, Stanier CO, Pandis SN. Coupled partitioning, dilution, and chemical aging of semivolatile organics. *Environ Sci Technol*. 2006;40:2635–2643. [PubMed: 16683603]
40. Watson AY, Bates RR, Kennedy D. *Transport and Uptake of Inhaled Gases*. Washington, DC: National Academies Press; 1988. <https://www.ncbi.nlm.nih.gov/books/NBK218139/>. Accessed November 14, 2017.
41. Patton JS, Byron PR. Inhaling medicines: delivering drugs to the body through the lungs. *Nat Rev Drug Discov*. 2007;6:nrd2153.
42. Tu KW, Knutson EO. Total deposition of ultrafine hydrophobic and hygroscopic aerosols in the human respiratory system. *Aerosol Sci Technol*. 1984;3:453–465.
43. Asgharian B. A model of deposition of hygroscopic particles in the human lung. *Aerosol Sci Technol*. 2004;38:938–947.
44. Varghese SK, Gangamma S. Particle deposition in human respiratory system: deposition of concentrated hygroscopic aerosols. *Inhal Toxicol*. 2009;21:619–630. [PubMed: 19459776]
45. Williams BJ, Goldstein AH, Kreisberg NM, Hering SV. An in-situ instrument for speciated organic composition of atmospheric aerosols: thermal desorption aerosol GC/MS-FID (TAG). *Aerosol Sci Technol*. 2006;40:627–638.
46. Williams BJ, Goldstein AH, Kreisberg NM, Hering SV. In situ measurements of gas/particle-phase transitions for atmospheric semivolatile organic compounds. *Proc Natl Acad Sci*. 2010;107:6676–6681. [PubMed: 20142511]
47. Paatero P. Least squares formulation of robust non-negative factor analysis. *Chemom Intell Lab Syst*. 1997;37:23–35.
48. Williams BJ, Goldstein AH, Millet DB, et al. Chemical speciation of organic aerosol during the International Consortium for Atmospheric Research on Transport and Transformation 2004: results from in situ measurements. *J Geophys Res Atmospheres*. 2007;112:D10S26.
49. Ulbrich IM, Canagaratna MR, Zhang Q, Worsnop DR, Jimenez JL. Interpretation of organic components from Positive Matrix Factorization of aerosol mass spectrometric data. *Atmos Chem Phys*. 2009;9:2891–2918.
50. Williams BJ, Goldstein AH, Kreisberg NM, et al. Major components of atmospheric organic aerosol in southern California as determined by hourly measurements of source marker compounds. *Atmos Chem Phys*. 2010;10:11577–11603.
51. Zhang Y, Williams BJ, Goldstein AH, Docherty K, Ulbrich IM, Jimenez JL. A technique for rapid gas chromatography analysis applied to ambient organic aerosol measurements from the thermal desorption aerosol gas chromatograph (TAG). *Aerosol Sci Technol*. 2014;48:1166–1182.
52. Zhang Y, Williams BJ, Goldstein AH, Docherty KS, Jimenez JL. A technique for rapid source apportionment applied to ambient organic aerosol measurements from a thermal desorption aerosol gas chromatograph (TAG). *Atmos Meas Tech*. 2016;9:5637–5653.
53. Lee JH, Hopke PK, Turner JR. Source identification of airborne PM_{2.5} at the St. Louis-Midwest Supersite. *J Geophys Res Atmospheres*. 2006;111. 10.1029/2005JD006329
54. Williams BJ, Zhang Y, Zuo X, et al. Organic and inorganic decomposition products from the thermal desorption of atmospheric particles. *Atmos Meas Tech*. 2016;9:1569–1586.
55. Kreidenweis SM, Petters MD, DeMott PJ. Single-parameter estimates of aerosol water content. *Environ Res Lett*. 2008;3:35002.
56. Duplissy J, DeCarlo PF, Dommen J, et al. Relating hygroscopicity and composition of organic aerosol particulate matter. *Atmospheric Chem Phys*. 2011;11:1155–1165.
57. Isaacman G, Kreisberg NM, Yee LD, et al. Online derivatization for hourly measurements of gas- and particle-phase semi-volatile oxygenated organic compounds by thermal desorption aerosol gas chromatography (SV-TAG). *Atmos Meas Tech*. 2014;7:4417–4429.
58. Kreisberg NM, Hering SV, Williams BJ, Worton DR, Goldstein AH. Quantification of hourly speciated organic compounds in atmospheric aerosols, measured by an in-situ thermal desorption aerosol gas chromatograph (TAG). *Aerosol Sci Technol*. 2009;43:38–52.
59. Huffman JA, Docherty KS, Aiken AC, et al. Chemically-resolved aerosol volatility measurements from two megacity field studies. *Atmos Chem Phys*. 2009;9:7161–7182.
60. Budisulistiorini SH, Nenes A, Carlton AG, Surratt JD, McNeill VF, Pye H. Simulating aqueous-phase isoprene-epoxydiol (IEPOX) secondary organic aerosol production during the 2013

- southern oxidant and aerosol study (SOAS). *Environ Sci Technol*. 2017;51:5026–5034. [PubMed: 28394569]
61. Hu WW, Campuzano-Jost P, Palm BB, et al. Characterization of a real-time tracer for isoprene epoxydiols-derived secondary organic aerosol (IEPOX-SOA) from aerosol mass spectrometer measurements. *Atmos Chem Phys*. 2015;15:11807–11833.
 62. Marais EA, Jacob DJ, Turner JR, Mickley LJ. Evidence of 1991–2013 decrease of biogenic secondary organic aerosol in response to SO₂ emission controls. *Environ Res Lett*. 2017;12:54018.
 63. Robinson NH, Hamilton JF, Allan JD, et al. Evidence for a significant proportion of Secondary Organic Aerosol from isoprene above a maritime tropical forest. *Atmos Chem Phys*. 2011;11:1039–1050.
 64. Isaacman-VanWertz G, Sueper DT, Aikin KC, et al. Automated single-ion peak fitting as an efficient approach for analyzing complex chromatographic data. *J Chromatogr A*. 2017;1529:81–92. [PubMed: 29126588]
 65. Shields HC, Fleischer DM, Weschler CJ. Comparisons among VOCs measured in three types of U.S. commercial buildings with different occupant densities. *Indoor Air*. 1996;6(1):2–17.
 66. Otake T, Yoshinaga J, Yanagisawa Y. Exposure to phthalate esters from indoor environment. *J Expo Anal Environ Epidemiol*. 2004;14:524–528. [PubMed: 15039795]
 67. Benning JL, Liu Z, Tiwari A, Little JC, Marr LC. Characterizing gas-particle interactions of phthalate plasticizer emitted from vinyl flooring. *Environ Sci Technol*. 2013;47:2696–2703. [PubMed: 23410053]
 68. R ži ková J, Raclavská H, Raclavský K, Juchelková D. Phthalates in PM_{2.5} airborne particles in the Moravian-Silesian Region, Czech Republic. *Perspect Sci*. 2016;7:178–183.
 69. Quintana-Belmares RO, Krais AM, Esfahani BK, et al. Phthalate esters on urban airborne particles: levels in PM₁₀ and PM_{2.5} from Mexico City and theoretical assessment of lung exposure. *Environ Res*. 2018;161:439–445. [PubMed: 29216490]
 70. Kusch P. Identification of Organic Additives in Nitrile Rubber Materials by Pyrolysis-GC-MS. <http://www.chromatographyonline.com/identification-organic-additives-nitrile-rubber-materials-pyrolysis-gc-ms-0?xml:id=&sk=&date=&pageID=3>. Accessed November 9, 2018.
 71. The Good Scents Company - Aromatic/Hydrocarbon/Inorganic Ingredients Catalog Information. <http://www.thegoodscentscompany.com/data/rw1061431.html>. Accessed January 8, 2019.
 72. ETHYLHEXYL BENZOATE, Skin Deep® Cosmetics Database, EWG. https://www.ewg.org/skindeep/ingredient/719014/ETHYLHEXYL_BENZOATE/. Accessed January 8, 2019.
 73. Ongwande M, Moonrinta R, Panyametheekul S, Tangbanluekal C, Morrison G. Concentrations and strengths of formaldehyde and acetaldehyde in office buildings in Bangkok, Thailand. *Indoor Built Environ*. 2009;18:569–575.
 74. Yamashita K, Noguchi M, Mizukoshi A, Yanagisawa Y. Acetaldehyde removal from indoor air through chemical absorption using L-cys-teine. *Int J Environ Res Public Health*. 2010;7:3489–3498. [PubMed: 20948938]
 75. Gupta KC, Ulsamer AG, Preuss PW. Formaldehyde in indoor air: sources and toxicity. *Environ Int*. 1982;8:349–358.
 76. Lovreglio P, Carrus A, Iavicoli S, Drago I, Persechino B, Soleo L. Indoor formaldehyde and acetaldehyde levels in the province of Bari, South Italy, and estimated health risk. *J Environ Monit*. 2009;11:955–961. [PubMed: 19436853]
 77. Kim H, Kim T, Hong W-H, Tanabe S. Concentration of formaldehyde, acetaldehyde, and five volatile organic compounds in indoor air: the clean-healthy house construction standard (South Korea). *J Asian Archit Build Eng*. 2017;16:633–639.
 78. Loeffroth G, Burton RM, Forehand L, et al. Characterization of environmental tobacco smoke. *Environ Sci Technol*. 1989;23:610–614.
 79. Jurvelin JA, Edwards RD, Vartiainen M, Pasanen P, Jantunen MJ. Residential indoor, outdoor, and workplace concentrations of carbonyl compounds: relationships with personal exposure concentrations and correlation with sources. *J Air Waste Manag Assoc*. 2003;53:560–573. [PubMed: 12774989]

80. Liu W, Zhang J, Zhang L, et al. Estimating contributions of indoor and outdoor sources to indoor carbonyl concentrations in three urban areas of the United States. *Atmos Environ.* 2006;40:2202–2214.
81. Klepac Pulani T, Busljeta I, Macan J, Plavec D, Turk R. Household chemicals - common cause of unintentional poisoning. *Arh Hig Rada Toksikol.* 2001;51:401–407.
82. Shah JJ, Singh HB. Distribution of volatile organic chemicals in outdoor and indoor air: a national VOCs data base. *Environ Sci Technol.* 1988;22:1381–1388. [PubMed: 22200458]
83. Weisel CP, Alimokhtari S, Sanders PF. Indoor air VOC concentrations in suburban and rural New Jersey. *Environ Sci Technol.* 2008;42:8231–8238. [PubMed: 19068799]
84. McDonald BC, de Gouw JA, Gilman JB, et al. Volatile chemical products emerging as largest petrochemical source of urban organic emissions. *Science.* 2018;359:760–764. [PubMed: 29449485]
85. Horii Y, Kannan K. Survey of organosilicone compounds, including cyclic and linear siloxanes, in personal-care and household products. *Arch Environ Contam Toxicol.* 2008;55(4):701–710. [PubMed: 18443842]
86. Wang R, Moody RP, Koniacki D, Zhu J. Low molecular weight cyclic volatile methylsiloxanes in cosmetic products sold in Canada: implication for dermal exposure. *Environ Int.* 2009;35:900–904. [PubMed: 19361861]
87. Lu Y, Yuan T, Wang W, Kannan K. Concentrations and assessment of exposure to siloxanes and synthetic musks in personal care products from China. *Environ Pollut Barking Essex.* 1987;2011(159):3522–3528.
88. Dudzina T, von Goetz N, Bogdal C, Biesterbos J, Hungerbühler K. Concentrations of cyclic volatile methylsiloxanes in European cosmetics and personal care products: prerequisite for human and environmental exposure assessment. *Environ Int.* 2014;62:86–94. [PubMed: 24184663]
89. Capela D, Alves A, Homem V, Santos L. From the shop to the drain - volatile methylsiloxanes in cosmetics and personal care products. *Environ Int.* 2016;92–93:50–62.
90. Janecek NJ, Hansen KM, Stanier CO. Comprehensive atmospheric modeling of reactive cyclic siloxanes and their oxidation products. *Atmospheric Chem Phys.* 2017;17:8357–8370.
91. Brown SK. Volatile organic pollutants in new and established buildings in Melbourne, Australia. *Indoor Air.* 2002;12:55–63. [PubMed: 11951711]
92. Huang Y, Ho S, Ho KF, Lee SC, Yu JZ, Louie P. Characteristics and health impacts of VOCs and carbonyls associated with residential cooking activities in Hong Kong. *J Hazard Mater.* 2011;186:344–351. [PubMed: 21112148]
93. Zhao P, Cheng Y-H, Lin C-C, Cheng Y-L. Effect of resin content and substrate on the emission of BTEX and carbonyls from low-VOC water-based wall paint. *Environ Sci Pollut Res Int.* 2016;23:3799–3808. [PubMed: 26498819]
94. Rogge WF, Hildemann LM, Mazurek MA, Cass GR, Simoneit B. Sources of fine organic aerosol. 2. Noncatalyst and catalyst-equipped automobiles and heavy-duty diesel trucks. *Environ Sci Technol.* 1993;27:636–651.
95. Erickson MH, Gueneron M, Jobson BT. Measuring long chain alkanes in diesel engine exhaust by thermal desorption PTR-MS. *Atmos Meas Tech.* 2014;7:225–239.
96. Chan A, Kreisberg NM, Hohaus T, et al. Speciated measurements of semivolatile and intermediate volatility organic compounds (S/IVOCs) in a pine forest during BEACHON-RoMBAS 2011. *Atmos Chem Phys.* 2016;16:1187–1205.
97. Hazrati S, Rostami R, Farjaminezhad M, Fazlzadeh M. Preliminary assessment of BTEX concentrations in indoor air of residential buildings and atmospheric ambient air in Ardabil, Iran. *Atmos Environ.* 2016;132:91–97.
98. Kruza M, Lewis AC, Morrison GC, Carslaw N. Impact of surface ozone interactions on indoor air chemistry: a modeling study. *Indoor Air.* 2017;27:1001–1011. [PubMed: 28303599]
99. Pekey B, Bozkurt ZB, Pekey H, et al. Indoor/outdoor concentrations and elemental composition of PM10/PM2.5 in urban/industrial areas of Kocaeli City, Turkey. *Indoor Air.* 2010;20:112–125. [PubMed: 20002793]
100. Chen C, Zhao B. Review of relationship between indoor and outdoor particles: I/O ratio, infiltration factor and penetration factor. *Atmos Environ.* 2011;45:275–288.

101. Viana M, Díez S, Reche C. Indoor and outdoor sources and infiltration processes of PM₁ and black carbon in an urban environment. *Atmos Environ*. 2011;45:6359–6367.
102. Oeder S, Dietrich S, Weichenmeier I, et al. Toxicity and elemental composition of particulate matter from outdoor and indoor air of elementary schools in Munich, Germany. *Indoor Air*. 2012;22:148–158. [PubMed: 21913995]
103. Sangiorgi G, Ferrero L, Ferrini BS, et al. Indoor airborne particle sources and semi-volatile partitioning effect of outdoor fine PM in offices. *Atmos Environ*. 2013;65:205–214.
104. Avery AM, Waring MS, DeCarlo PF. Seasonal variation in aerosol composition and concentration upon transport from the outdoor to indoor environment. *Environ Sci Process Impacts*. 2019;21:528–547. [PubMed: 30698188]
105. Yocom JE. A critical review. *J Air Pollut Control Assoc*. 1982;32:500–520.
106. Marais EA, Jacob DJ, Jimenez JL, et al. Aqueous-phase mechanism for secondary organic aerosol formation from isoprene: application to the southeast United States and co-benefit of SO₂ emission controls. *Atmos Chem Phys*. 2016;16:1603–1618. [PubMed: 32742280]
107. Surratt JD, Kroll JH, Kleindienst TE, et al. Evidence for organosulfates in secondary organic aerosol. *Environ Sci Technol*. 2007;41:517–527. [PubMed: 17310716]
108. Eddingsaas NC, VanderVelde DG, Wennberg PO. Kinetics and products of the acid-catalyzed ring-opening of atmospherically relevant butyl epoxy alcohols. *J Phys Chem A*. 2010;114:8106–8113. [PubMed: 20684583]
109. Lin Y-H, Zhang Z, Docherty KS, et al. Isoprene epoxydiols as precursors to secondary organic aerosol formation: acid-catalyzed reactive uptake studies with authentic compounds. *Environ Sci Technol*. 2012;46:250–258. [PubMed: 22103348]
110. Lin Y-H, Knipping EM, Edgerton ES, Shaw SL, Surratt JD. Investigating the influences of SO₂ and NH₃ levels on isoprene-derived secondary organic aerosol formation using conditional sampling approaches. *Atmospheric Chem Phys*. 2013;13:8457–8470.
111. Budisulistiorini SH, Li X, Bairai ST, et al. Examining the effects of anthropogenic emissions on isoprene-derived secondary organic aerosol formation during the 2013 Southern Oxidant and Aerosol Study (SOAS) at the Look Rock, Tennessee ground site. *Atmospheric Chem Phys*. 2015;15:8871–8888.
112. Chakraborty A, Gupta T, Tripathi SN. Chemical composition and characteristics of ambient aerosols and rainwater residues during Indian summer monsoon: insight from aerosol mass spectrometry. *Atmos Environ*. 2016;136:144–155.
113. Guo L-C, Zhang Y, Lin H, et al. The washout effects of rainfall on atmospheric particulate pollution in two Chinese cities. *Environ Pollut*. 2016;215:195–202. [PubMed: 27203467]
114. Weschler CJ. Ozone in indoor environments: concentration and chemistry. *Indoor Air*. 2000;10:269–288. [PubMed: 11089331]
115. Morrison GC, Nazaroff WW. The rate of ozone uptake on carpets: experimental studies. *Environ Sci Technol*. 2000;34:4963–4968.
116. Wang H, Morrison G. Ozone-surface reactions in five homes: surface reaction probabilities, aldehyde yields, and trends. *Indoor Air*. 2010;20:224–234. [PubMed: 20408899]
117. Fabbri D, Torri C, Simoneit B, Marynowski L, Rushdi AI, Fabianka MJ. Levoglucosan and other cellulose and lignin markers in emissions from burning of Miocene lignites. *Atmos Environ*. 2009;43:2286–2295.
118. Simoneit B, Schauer JJ, Nolte CG, et al. Levoglucosan, a tracer for cellulose in biomass burning and atmospheric particles. *Atmos Environ*. 1999;33:173–182.
119. Fraser MP, Lakshmanan K. Using levoglucosan as a molecular marker for the long-range transport of biomass combustion aerosols. *Environ Sci Technol*. 2000;34:4560–4564.
120. Hennigan CJ, Sullivan AP, Collett JL, Robinson AL. Levoglucosan stability in biomass burning particles exposed to hydroxyl radicals. *Geophys Res Lett*. 2010;37. 10.1029/2010GL043088
121. Kessler SH, Smith JD, Che DL, Worsnop DR, Wilson KR, Kroll JH. Chemical sinks of organic aerosol: kinetics and products of the heterogeneous oxidation of erythritol and levoglucosan. *Environ Sci Technol*. 2010;44:7005–7010. [PubMed: 20707414]
122. Garbe L-A, Lange H, Tressl R. Biosynthesis of γ -nonalactone in yeast. In: Takeoka Gary R., Güntert Matthias, Engel Karl-Heinz, ed. *Aroma Active Compounds in Foods*. Vol 794.

ACS Symposium Series. Washington, DC: American Chemical Society; 2001:176–182. 10.1021/bk-2001-0794.ch014

123. Poisson L, Schieberle P. Characterization of the most odor-active compounds in an American Bourbon whisky by application of the aroma extract dilution analysis. *J Agric Food Chem.* 2008;56:5813–5819. [PubMed: 18570373]
124. Chen J, Zhu Y. *Solid State Fermentation for Foods and Beverages.* Boca Raton, FL: CRC Press; 2013.
125. Socol CR, Pandey A, Larroche C. *Fermentation Processes Engineering in the Food Industry.* Boca Raton, FL: CRC Press; 2013.
126. Ramalho O, Moularat S, Horn W, Knudsen H, Wargocki P, Muller B. Occurrence of odorous compounds in the emission of building materials measured by GC-olfactometry. July 2009.726, 2009. https://hal.archives-ouvertes.fr/hal-00701721/file/Poster_GCO_low.pdf. Accessed November 28, 2018.
127. Fuselli S, De Felice M, Morlino R, Turrio-Baldassarri L. A three year study on 14 VOCs at one site in Rome: levels, seasonal variations, indoor/outdoor ratio and temporal trends. *Int J Environ Res Public Health.* 2010;7:3792–3803. [PubMed: 21139860]
128. Boor BE, Järnström H, Novoselac A, Xu Y. Infant exposure to emissions of volatile organic compounds from crib mattresses. *Environ Sci Technol.* 2014;48:3541–3549. [PubMed: 24548111]
129. Pubchem. Diethyltoluamide. <https://pubchem.ncbi.nlm.nih.gov/compound/4284>. Accessed January 9, 2019.
130. Hedione. <https://www.perfumersworld.com/product/hedione-3JJ00218>. Accessed January 9, 2019.
131. Sarantis HV, Naidenko O, Gray S, et al. Not So Sexy: The Health Risks of Secret Chemicals in Fragrance; 2018.
132. Salthammer T. Emissions of volatile organic compounds from products and materials in indoor environments. In: Plushke P, ed. *Indoor Air Pollution: Part F (The Handbook of Environmental Chemistry)*. Berlin, Germany: Springer Science & Business Media; 2004:37–71. <https://books.google.com/books?xml:id=GXwII8L7aosC>
133. Meciariova L, Vilcekova S. Determination of VOCs in the indoor air of a new and a renovated apartment. *Sel Sci Pap - J Civ Eng.* 2016;11:107–118.
134. Jo W-K, Lee J-H, Lim H-J, Jeong W-S. Naphthalene emissions from moth repellents or toilet deodorant blocks determined using headspace and small-chamber tests. *J Environ Sci.* 2008;20:1012–1017.
135. Clausen PA, Liu Z, Xu Y, Kofoed-Sørensen V, Little JC. Influence of air flow rate on emission of DEHP from vinyl flooring in the emission cell FLEC: measurements and CFD simulation. *Atmos Environ.* 2010;44:2760–2766.
136. Liang Y, Caillot O, Zhang J, Zhu J, Xu Y. Large-scale chamber investigation and simulation of phthalate emissions from vinyl flooring. *Build Environ.* 2015;89:141–149.
137. Liang Y, Xu Y. The influence of surface sorption and air flow rate on phthalate emissions from vinyl flooring: measurement and modeling. *Atmos Environ.* 2015;103:147–155.
138. Wei W, Mandin C, Ramalho O. Influence of indoor environmental factors on mass transfer parameters and concentrations of semi-volatile organic compounds. *Chemosphere.* 2018;195:223–235. [PubMed: 29268180]
139. Deng B, Kim CN. An analytical model for VOCs emission from dry building materials. *Atmos Environ.* 2004;38:1173–1180.
140. Liagkouridis I, Cousins IT, Cousins AP. Emissions and fate of brominated flame retardants in the indoor environment: a critical review of modelling approaches. *Sci Total Environ.* 2014;491–492:87–99.
141. Weschler CJ, Hodgson AT, Wooley JD. Indoor chemistry: ozone, volatile organic compounds, and carpets. *Environ Sci Technol.* 1992;26:2371–2377.
142. Wang H, Morrison GC. Ozone-initiated secondary emission rates of aldehydes from indoor surfaces in four homes. *Environ Sci Technol.* 2006;40:5263–5268. [PubMed: 16999097]

143. Saarela K. Emission from floor coverings. In: Salthammer T, ed. *Organic Indoor Air Pollutants: Occurrence, Measurement, Evaluation*. Hoboken, NJ:Wiley; 2008:191–202. <https://books.google.com/books?xml:id=k9QaGRQDPo4C>
144. Morrison GC, Nazaroff WW. Ozone interactions with carpet: secondary emissions of aldehydes. *Environ Sci Technol*. 2002;36:2185–2192. [PubMed: 12038828]
145. Kamens R, Jang M, Chien C-J, Leach K. Aerosol formation from the reaction of α -pinene and ozone using a gas-phase kinetics-aerosol partitioning model. *Environ Sci Technol*. 1999;33:1430–1438.
146. Venkatachari P, Hopke PK. Characterization of products formed in the reaction of ozone with alpha-pinene: case for organic peroxides. *J Environ Monit JEM*. 2008;10:966–974. [PubMed: 18688467]
147. Carslaw N. A mechanistic study of limonene oxidation products and pathways following cleaning activities. *Atmos Environ*. 2013;80:507–513.
148. Zhang X, McVay RC, Huang DD, et al. Formation and evolution of molecular products in α -pinene secondary organic aerosol. *Proc Natl Acad Sci U S A*. 2015;112:14168–14173. [PubMed: 26578760]
149. Witkowski B, Gierczak T. Characterization of the limonene oxidation products with liquid chromatography coupled to the tandem mass spectrometry. *Atmos Environ*. 2017;154:297–307.
150. Coleman BK, Destailats H, Hodgson AT, Nazaroff WW. Ozone consumption and volatile byproduct formation from surface reactions with aircraft cabin materials and clothing fabrics. *Atmos Environ*. 2008;42:642–654.
151. Rai AC, Guo B, Lin C-H, Zhang J, Pei J, Chen Q. Ozone reaction with clothing and its initiated VOC emissions in an environmental chamber. *Indoor Air*. 2014;24:49–58. [PubMed: 23841649]

Practical Implications

- Natural ventilation influences indoor concentrations of particle- and gas-phase organic pollutants via five distinct chemical and/or physical mechanisms.
- The contribution of each mechanism to total indoor air quality depends on factors including outdoor pollutant concentrations, air exchange rates, and surface films present inside the home.
- Occupant window-opening behavior is influenced by desired temperature control or perceived air quality modifications, and we find that while window opening can diminish some indoor-originating pollutants, it can simultaneously increase emission rates of semi- and intermediately volatile species and oxidation products.

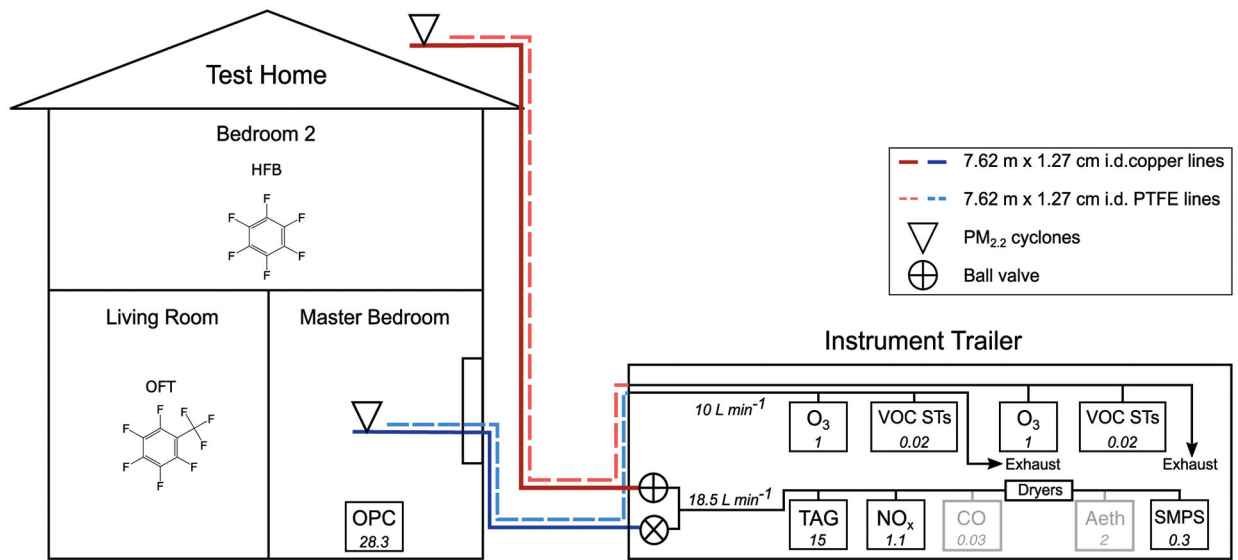


FIGURE 1.

Diagram of experimental setup. Instruments with gray outlines and text collected data that are not provided in this manuscript and are included in the figure primarily to illustrate balanced flows. Flow rates (L min^{-1}) are included for each instrument in italicized text

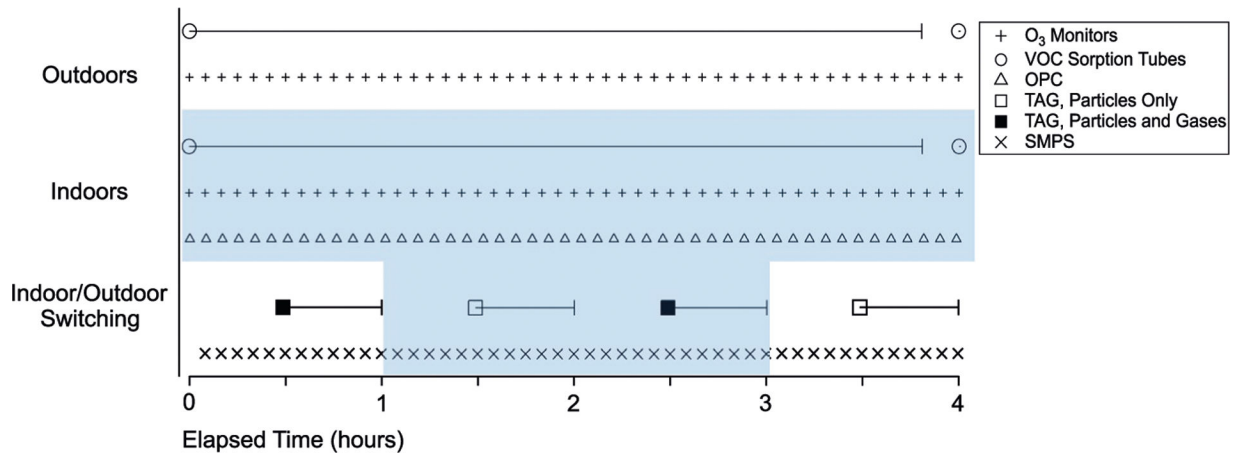


FIGURE 2. Illustration of sampling schedule over a 4-h period. Instrument sampling resolutions are provided in Table 1. The blue shaded region denotes indoor sampling periods

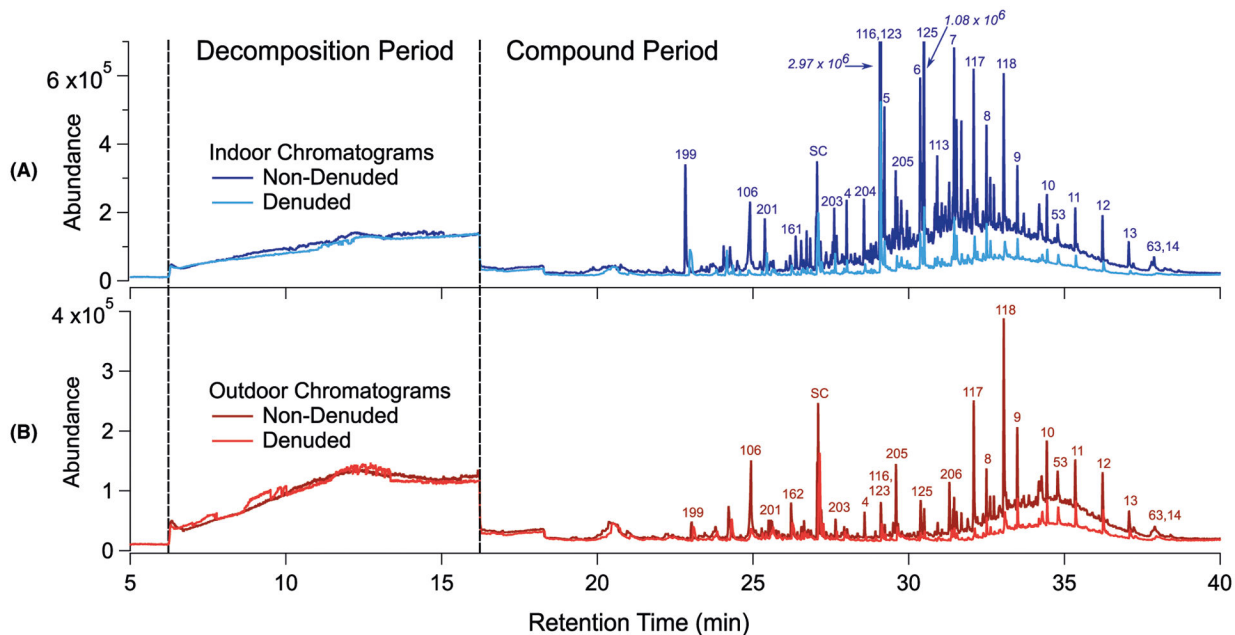


FIGURE 3.

Example total ion chromatograms obtained during the WC sampling period: (A) indoor non-denuded and denuded chromatograms, and (B) outdoor non-denuded and denuded chromatograms. All four chromatograms were collected within a 4-h time span. Note the higher abundance scale (y -axis) for indoor samples. Selected compounds are labeled with numbers, which correspond to numbered compounds in Table S2. *Italicized numbers* correspond to higher peak abundances that exceed the y -axis range

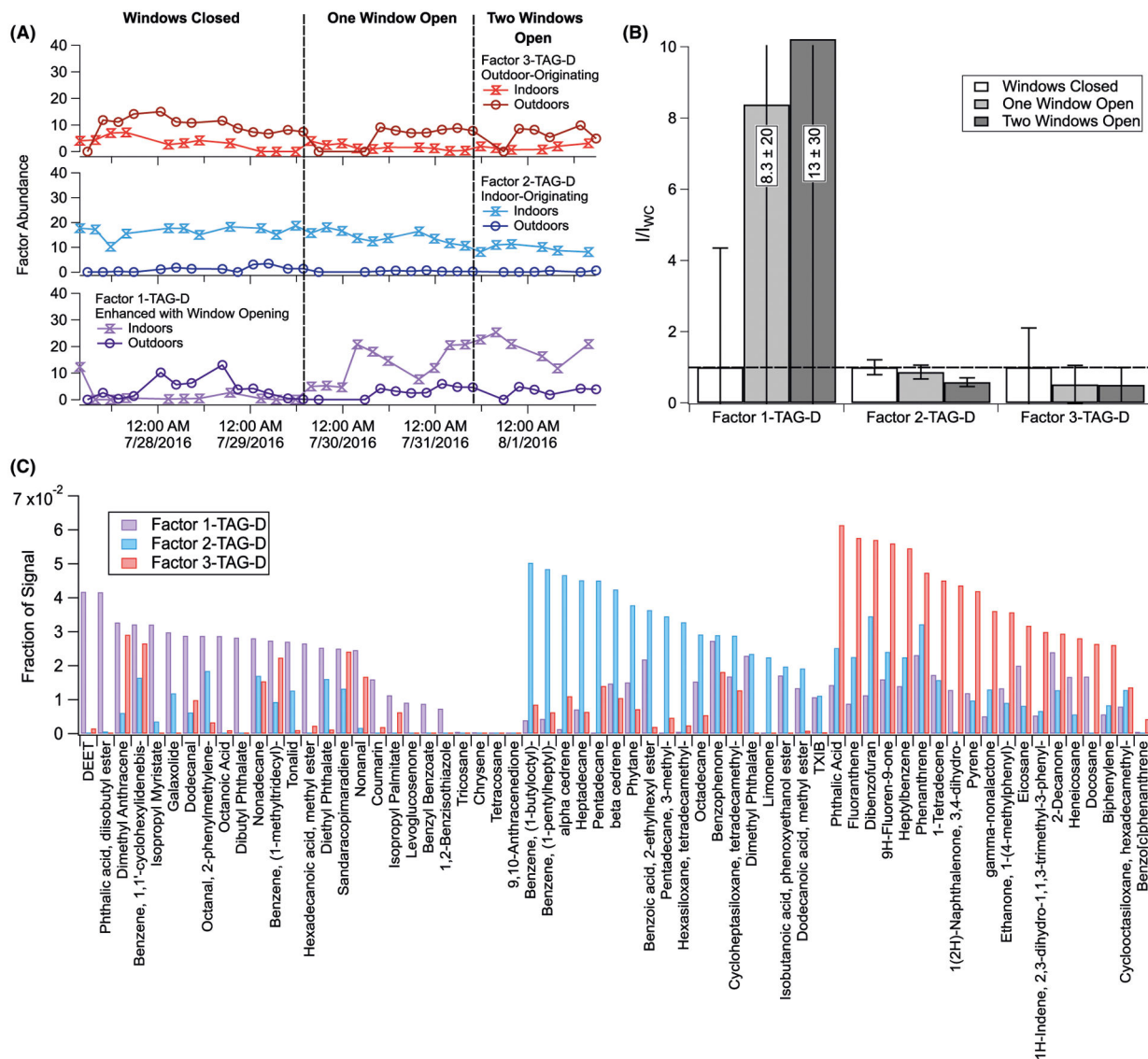


FIGURE 4. Three-factor PMF solution for denuded (particles only) TAG integrated compounds. Analysis details are provided in Section S4. Shown here are (A) time series for each of the three factors, split into indoor and outdoor chromatograms; (B) indoor chromatogram factor abundances normalized to windows closed conditions (I/I_{WC}) for each factor; and (C) compound factor loadings (see Table S3)

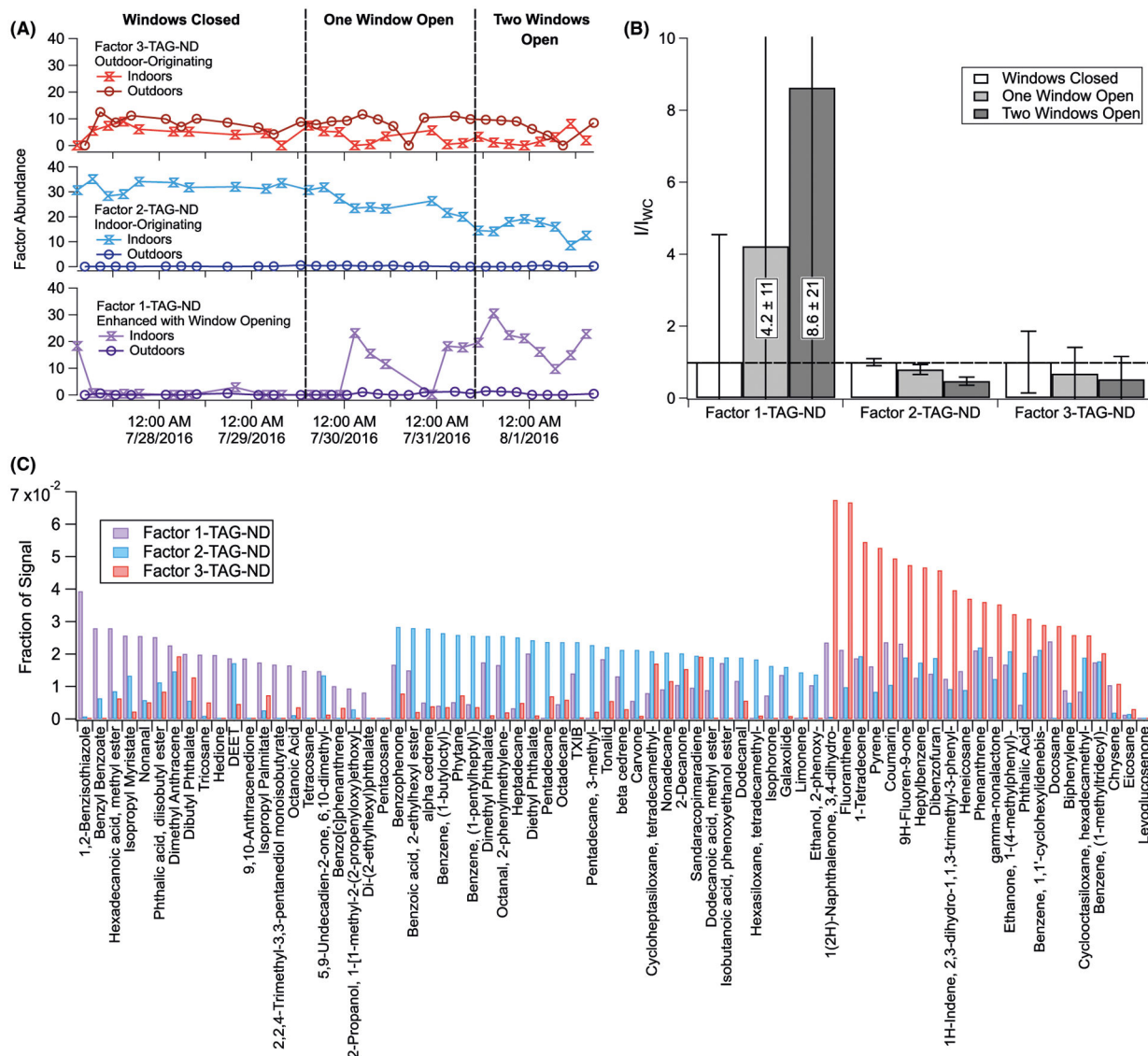


FIGURE 5. Three-factor PMF solution for non-denuded (particles and partial gases) TAG integrated compounds. Analysis details are provided in Section S4. Shown here are (A) time series for each of the three factors, split into indoor and outdoor chromatograms; (B) indoor chromatogram factor abundances normalized to windows closed conditions (I/I_{WC}) for each factor; and (C) compound factor loadings (see Table S4)

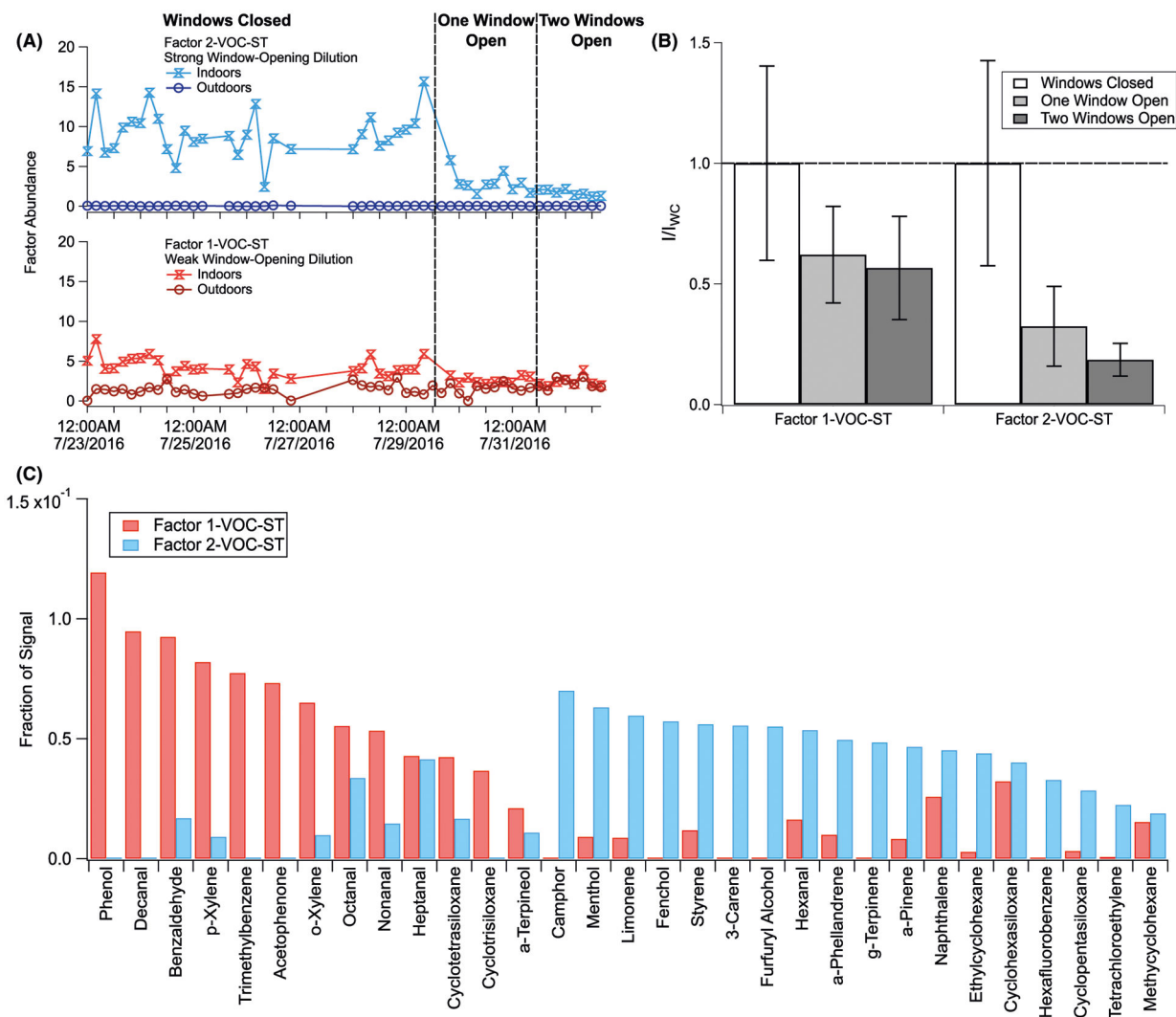


FIGURE 6. Two-factor PMF solution for VOC adsorbent tube integrated compounds. Analysis details are provided in Section S4. Shown here are (A) time series for each of the two factors, split into indoor and outdoor chromatograms; (B) indoor chromatogram factor abundances normalized to windows closed conditions (I/I_{WC}) for each factor; and (C) compound factor loadings (see Table S5)

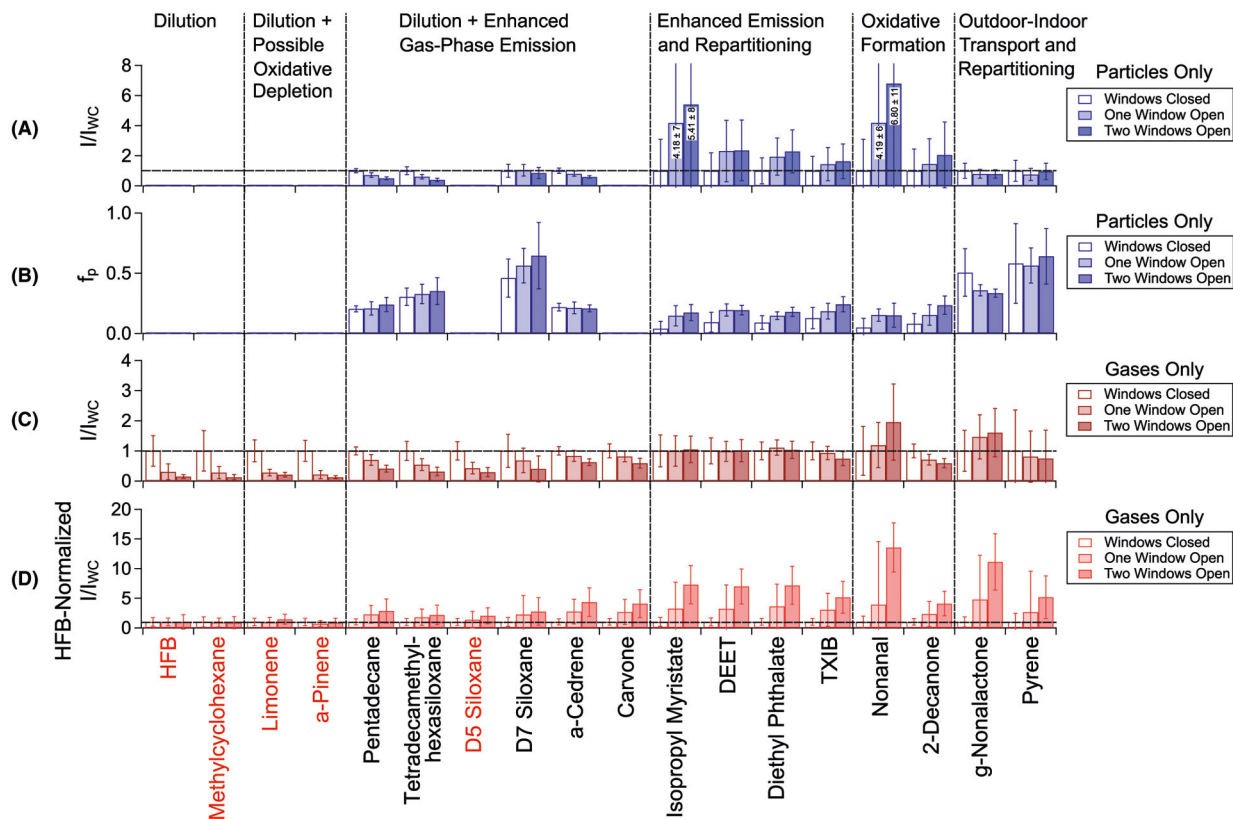


FIGURE 7. Indoor changes observed for selected TAG compounds (indicated with black text) and VOC adsorbent tube compounds (indicated with red text) across the three natural ventilation conditions. Shown are (A) the particle-only fraction of TAG compounds (denuded abundances) normalized to WC conditions; (B) approximate f_p for TAG compounds, calculated as the ratio of average denuded (particle) to average non-denuded (particle + gas) abundances; (C) gas-phase values for VOCs and the gas fraction of TAG compounds, approximated as non-denuded (particle + gas) minus denuded (particle); and (D) approximate indoor gases normalized to the indoor tracer molecule HFB I/I_{WC} at each ventilation condition, effectively correcting for altered air exchange with window opening

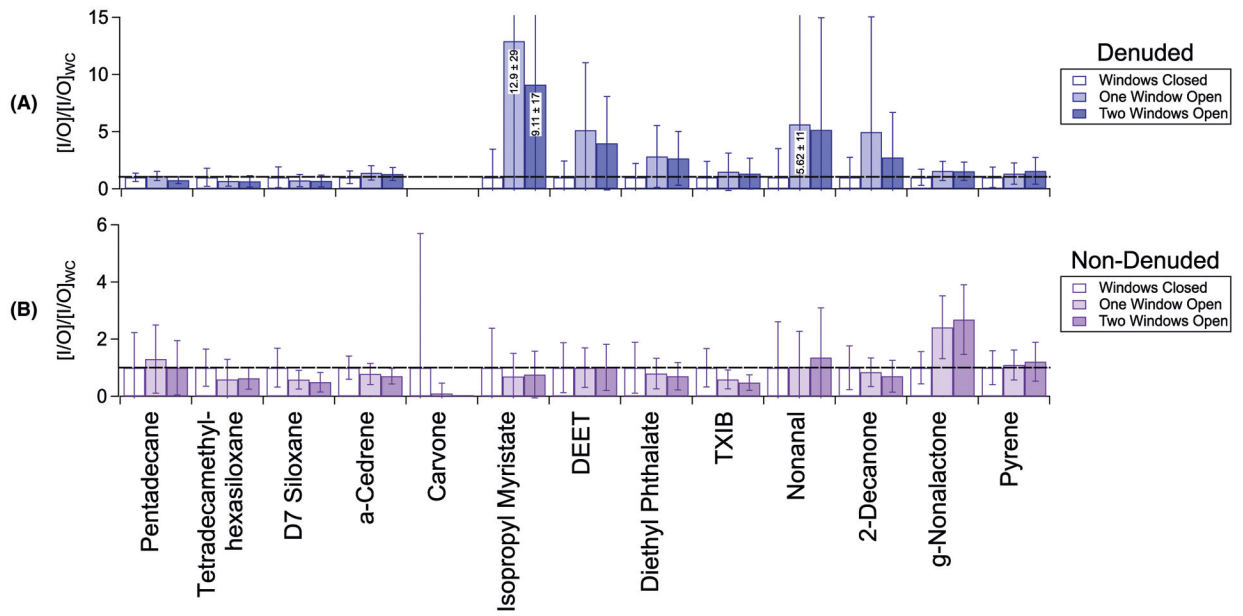


FIGURE 8.

Indoor-to-outdoor ratios, normalized to windows closed conditions ($[I/O]/[I/O]_{WC}$) for selected TAG compounds across the three natural ventilation conditions: (A) particles only (denuded abundances); (B) particles and gases (non-denuded abundances)

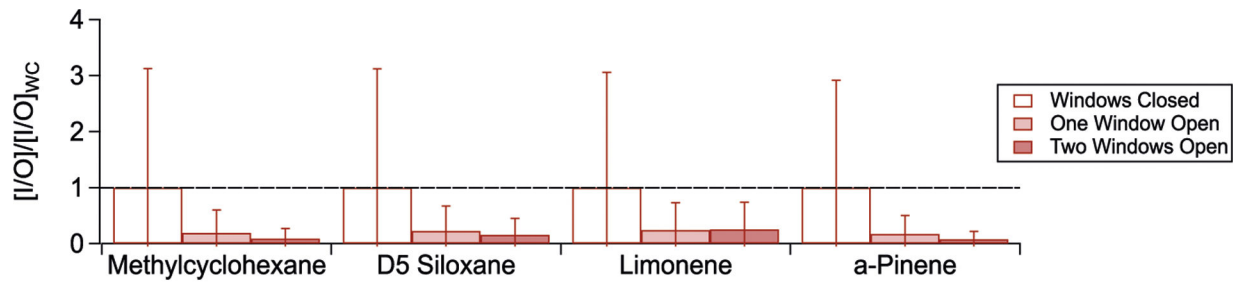


FIGURE 9.

Indoor-to-outdoor ratios, normalized to windows closed conditions ($[I/O]_{WC}$) for selected VOC adsorbent tube compounds across the three natural ventilation conditions

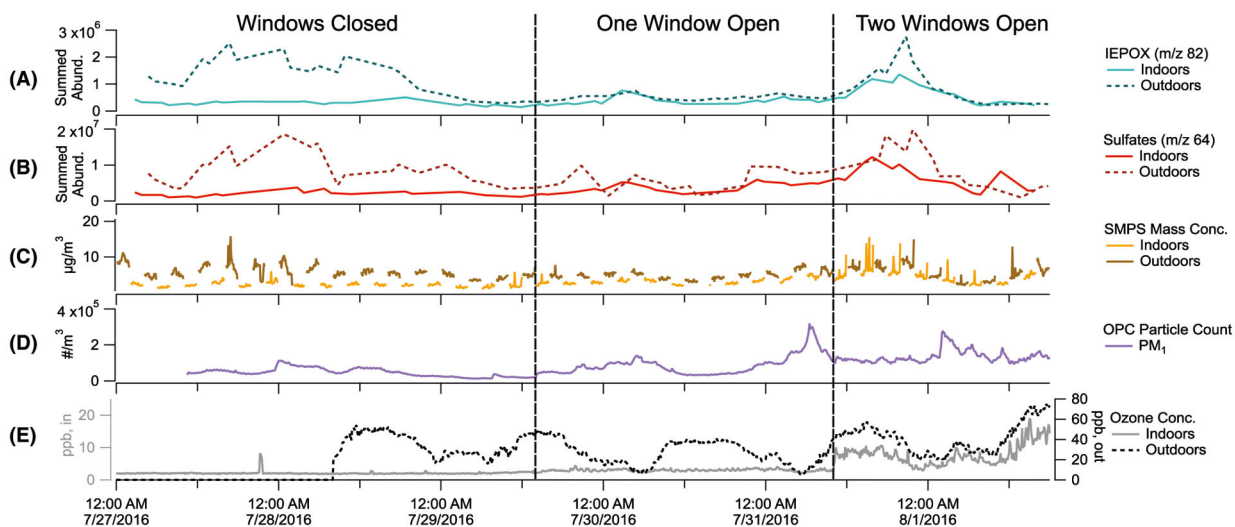


FIGURE 10. Indoor and outdoor time series for key species measured throughout the study: (A) integrated m/z 82 TAG decomposition abundances, a marker for IEPOX aerosol; (B) integrated m/z 64 TAG decomposition abundance, a marker for sulfate aerosol; (C) SMPS-measured total mass concentrations, assuming spherical particles and densities of 1.2 g cm^{-3} ; (D) Indoor OPC-measured PM_{10} particle number concentrations; and (E) O_3 concentrations (lower indoor concentrations on primary y -axis and higher outdoor concentrations on secondary y -axis)

TABLE 1

Description of measurements, sampling location, and resolution for each instrument

Instrument	Measurements	Sampling location	Sampling resolution (min)
TAG	Molecular-level speciation of organic particles and some gases (S/VOC)	Indoor/Outdoor switching	60
SMPS	Particle size distributions and concentrations	Indoor/Outdoor switching	5
NO _x (NO-NO ₂) Monitor	Trace-level NO _x (NO and NO ₂) concentrations	Indoor/Outdoor switching	1
O ₃ Monitors	Trace-level O ₃ concentrations	Indoors and outdoors	5
VOC Adsorbent Tubes	Molecular-level speciation of organic gases (VOC)	Indoors and outdoors	240
OPC	Indoor particle number concentrations	Indoors only	5